CircFAM114A2 Inhibits Bladder Cancer Proliferation and Promotes Cisplatin Sensitivity via the miR-222-3p/P27 and miR-146a-5p/P21 Cascades

Jiancheng Lu
The first affiliated hospital of Nanjing medical university
Zijian Zhou
The first affiliated hospital of Nanjing medical university
Jingzi Wang
The first affiliated hospital of Nanjing medical university
Xiao Yang
The first affiliated hospital of Nanjing medical university
Hao Yu
The First Affiliated Hospital of Nanjing Medical University
Jie Han
The first affiliated hospital of Nanjing medical university
Dexiang Feng
The First Affiliated Hospital of Nanjing Medical University
Baorui Yuan
The First Affiliated Hospital of Nanjing Medical University
Qikai Wu
The first affiliated hospital of Nanjing medical university
Pengchao Li
The first affiliated hospital of Nanjing medical university
Qiang Lu
The first affiliated hospital of Nanjing medical university
Haiwei Yang (haiweiyang@njmu.edu.cn)
The First Affiliated Hospital of Nanjing Medical University https://orcid.org/0000-0001-8984-5007

Research

Keywords: Bladder cancer, circular RNA, micro RNA, proliferation, chemosensitivity

Posted Date: November 12th, 2020

DOI: https://doi.org/10.21203/rs.3.rs-103659/v1

Abstract

Background: Circular RNAs (circRNAs) are noncoding RNAs that have the structure of a covalently closed loop. Increasing data has proved that circRNA can influence the development and progression of tumors. CircFAM114A2 is generated from several exons of FAM114A2. However, the function and mechanisms of circFAM114A2 in bladder cancer (BCa) remain unclear.

Methods: Here, to elucidate the potential roles of circFAM114A2 in BCa, we conducted RNA-sequencing on 5 pairs of BCa samples and screened for circRNAs. CircRNAs, microRNAs (miRNAs) and mRNAs, as well as levels of P27 and P21, in human cells and tissues were detected by qRT-PCR and western blot, respectively. CircRNA-miRNA interactions and miRNA-downstream mRNAs interactions were investigated by RNA pull-down assay and fluorescence in situ hybridization (FISH) or luciferase reporter assays, respectively. Then, the function of circFAM114A2 in BCa was explored using cell proliferation, cell cycle and tumorigenesis assays in nude mice. Finally, the function of circFAM114A2 in cisplatin chemo-sensitivity in BCa was detected by IC50 and tumor formation of xenograft in cisplatin-treated nude mice.

Results: We discovered that circFAM114A2 levels were decreased in BCa cell lines and tissues. According to follow-up data, BCa patients with higher circFAM114A2 expression had better survival. Importantly, the levels of circFAM114A2 were associated with the histological grade of BCa. Overexpression of circFAM114A2 inhibited cell proliferation and increased sensitivity to cisplatin chemotherapy. Mechanistically, circFAM114A2 directly sponged miR-222-3p/miR-146a-5p and subsequently influenced the expression of the downstream target genes P27/P21, which, in turn, inhibited progression of BCa.

Conclusion: In conclusion, **c**ircFAM114A2 acted as a tumor suppressor through a novel circFAM114A2/miR-222-3p/P27 and circFAM114A2/miR-146a-5p/P21 pathway. CircFAM1142 has therefore great potential as a prognostic biomarker and therapeutic target for BCa.

Background

Bladder cancer (BCa) has the highest incidence in the urinary system with a high morbidity and mortality worldwide (1). Depending on the depth of tumor invasion, BCa is categorized into either muscle-invasive (MIBC) (20 ~ 30%) and non-muscle invasive tumor (NMIBC) (70 ~ 80%) (2). Currently, the most common treatments for BCa are surgery, chemotherapy and radiotherapy. However, the recurrence rate is still very high, and the 5-year BCa-specific survival is inadequate (3). For MIBC, its overall efficiency is only approximately 35%, despite using adjuvant chemotherapy or neoadjuvant chemotherapy based on cisplatin (4, 5). Therefore, more research on molecular mechanisms of chemotherapy-resistance is needed, which may provide new insights about the diagnosis and therapy of BCa.

Circular RNA (circRNA) is a new type of noncoding RNA (ncRNA) and consists of a covalent closed-loop assembly minus the 3' poly A tail and 5’ cap (6). Largely, circRNAs can be organized into five classes: circRNAs from introns, intergenic circRNAs, exonic circRNAs, exon-intron circRNAs, and antisense circRNAs (7), which are generated from diverse mechanisms including exon skipping, intron pairing and

RNA-binding proteins (8). Recently, studies have discovered that circRNAs are intimately related to the incidence and establishment of tumors (7, 9–11). CircRNAs can perform as competitive endogenous RNAs (ceRNAs) and protect the target mRNA from degradation by sponging microRNA (miRNA) (12). MiRNAs are non-coding RNAs that are 19–25 nucleotides in length and have the capability to influence various ranges of biological functions through regulating the expression of mRNAs (13). MiRNAs play an important function in facilitating or repressing carcinogenesis, development and metastasis in BCa (14, 15). CircRNAs can directly bind to miRNAs, which play a role as 'miRNA sponges' and cease the regulation of target mRNAs (11, 16). Yang et al. reported that circITCH could inhibit progression of BCa through a circITCH/miR-17 or miR-224/P21 or PTEN pathway (17). CircSLC8A1 was shown to also inhibit progression of BCa via circSLC8A1/miR-130b or miR-494/PTEN pathway (18). Nevertheless, the biological properties of circRNAs in BCa remain mainly unidentified and need further research. To assess the role of circRNAs in the tumorigenesis and formation of BCa, our group conducted RNA sequencing on five pairs of BCa tissues in 2017 (19) and found that circFAM114A2 was one of three most down-regulated circRNAs. CircFAM114A2 has a much higher tissue average read count than the other two most down-regulated circRNAs. CircFAM114A2 is formed by several exons of the FAM114A2 gene. The underlying function and mechanisms of circFAM114A2 in BCa are still unclear.

Cisplatin has always been a major part of the chemotherapy regimen among patients with BCa. The long-term survival of patients is greatly hindered through chemotherapy resistance to cisplatin (20). Therefore, there is a need for more studies to reveal the mechanisms of cisplatin resistance. According to various studies, cell cycle regulation and cell apoptosis are the theoretical basis of cisplatin action and play important roles in cisplatin chemotherapy resistance (21, 22). P27 and P21 are classic tumor suppressors as they play a crucial function in regulating cell cycle transition (23, 24). Ripani et al. reported that P27 induces cell cycle arrest and increases the sensitivity of colon carcinoma cell to cisplatin (25). Wang et al. reported that P21 could promote cell cycle arrest and increase the cisplatin sensitivity of BCa (26).

In our study, we discovered that: 1) circFAM114A2 was decreased in BCa versus normal tissue and related to prognosis of BCa patients; 2) circFAM114A2 could inhibit BCa cells proliferation and sensitize BCa cells to cisplatin; 3) circFAM114A2 affected the expression of P27 and P21 by sponging miR-222-3p and miR-146a-5p. On the whole, circFAM114A2 can function as a possible biomarker and potential target for BCa diagnosis and therapy.

Methods

Clinical specimens and cell lines

BCa tumor tissues and healthy tissues were acquired through BCa patients who underwent an operation at the first affiliated hospital of Nanjing Medical University from 2013 to 2017. Tumor tissue is the tissue pathologically diagnosed as BCa, and adjacent normal tissue is the healthy tissue without tumor which near the tumor tissue more than 5cm in the same patient. Overall, 46 paired BCa tissues were frozen in liquid nitrogen and stowed at −80°C. Utilization of tissues was granted approval by the ethics board at

the hospital. Participants were asked to sign informed consent before using clinical resources. Furthermore, a group of 46 BCa patients with clinical-pathological characteristics were monitored. The monitoring period varied between 1 to 62.5 months. Follow-up period was initiated on the day of the operation and lasted until time of disease advancement. The study methodologies conformed to the standards set by the Declaration of Helsinki. The BCa lines (SV-HUC, BIU87, TCC, T24, RT4, 5637, 253J, UMUC3 and J82) were acquired through the Type Culture Collection of the Chinese Academy of Sciences (Shanghai, China). And we listed a brief introduction to the background of these cell lines in Additional table 1. Cells were maintained in DMEM with 10% FBS in a 37°C incubator with 5% CO2.

Transfection

The stable transfection was used in circFAM114A2 relative transfection. Lentivirus constructs containing circFAM114A2 overexpression or knockdown was acquired through OBIO (Obio Technology Corp, China). T24 and 5637 BCa cells were placed in 6-well plates. Cells were then transfected with siRNA (si circFAM114A2-1, si circFAM114A2-2), knockdown negative control (si NC), overexpression lentivirus construct (circFAM114A2) and overexpression negative control (vector) at 50% confluency. The infected cells were treated with puromycin (4μg/ml) for two weeks. The transient transfection method was used in miRNAs relative transfection. The miRNA mimics and controls utilized for transfection were bought through Ribobio (Guangzhou, China). The procedure was conducted with the Lipofectamine 3000 kit (Invitrogen, USA) as per established guidelines (27).

RNA isolation and quantitative Real Time-PCR (qRT-PCR)

RNA was extracted through cells and tissues with Trizol as per established guidelines. Relative cDNA was produced by utilizing HiScript (Vazyme, China). LightCycler 480 (Roche, USA) was used for qRT-PCR of the circRNA and miRNAs. U6 and β-actin were selected as controls for circRNA, miRNA and mRNA identification. The CT values of target RNA were normalized by subtracting the CT value of β-actin. Every experiment was conducted three times and results were assessed through comparison of CT values. PCR primers were bought through Tsingke (Beijing, China) and listed in additional table 2.

Protein extraction and Western blotting

The cells were lysed using RIPA buffer that contained protease inhibitors (Sigma, USA). Protein was collected and measured using bicinchoninic acid (BCA) assessment. Protein was isolated using 10% SDS-PAGE and moved onto polyvinylidene fluoride (PVDF) membranes. Membrane was incubated with P27 (1:5000, Abcam, USA), P21 (1:5000, Abcam, USA) or β-actin (1:5000, Proteintech, USA) primary antibody. Next, membranes were treated with peroxidase (HRP)-conjugated anti-rabbit secondary antibody (1:1000, Cell Signaling Technology, USA). After conducting washes, proteins were identified utilizing chemiluminescence and assessed with Image Lab (Bio-Rad, USA).

Evaluation of cell proliferation and cloning formation

To evaluate cell growth, transfected T24 or 5637 BCa cells were placed in 96-well plates with 2000 or 4000 cells respectively per well. At 24, 48, 72 and 96h post-seeding, cell viability was calculated through the cell counting kit-8 (CCK-8) system as per established guidelines. In summary, 10 µl CCK-8 reagents were put into each well and the plate was placed at 37 °C for 1h in the dark. Absorbance was quantified (450 nm) using a microplate reader (Tecan, Switzerland).

To evaluate colony formation, cells were placed in 6-well plates at 500 or 1000 cells/well and cultured in DMEM with 10% FBS for two weeks. Post-fixation by methanol, cells were stained using 0.1% crystal violet for 30 min. Colonies were visualized and calculated.

IC50 determination

The transfected T24 or 5637 BCa cells were gathered and placed in 96-well plate at 5000 cells/well. After an overnight incubation, a series of dilute concentrations of cisplatin (128, 64, 50, 40, 32, 16, 8, 4, 2, and 1 µM, Sigma, USA) were added to the transfected cells for 24h. Next, viability was quantified by CCK-8 technique as per established protocol. IC50 was generated with the probit regression model (28). Analyses were replicated three times.

Evaluation of cell cycle and apoptosis

To evaluate cell cycle, transfected BCa cells were stained with the cycle test and DNA reagent kit (BD Biosciences, USA) and quantified through flow cytometry (Becton Dickinson, USA). Cell proportion in G0/1, S and G2/M phases were analyzed by Modifit software (Version 5.0). To identify apoptosis, cells were stained by annexin V-APC/7AAD apoptosis kit (eBiosciences, USA) and assessed utilizing flow cytometry. To investigate the apoptotic rate of BCa cells treated with cisplatin, BCa cells at 70% confluence were treated with 4 µmol/ml cisplatin for 24h and then collected for follow-up apoptosis testing.

Biotin-coupled miRNA capture

About 2×10^6 BCa cells at 50% confluence were transfected using 50 µM biotinylated miRNA mimics or nonsense control (NC) (Ribobio Guangzhou, China). After 24h, cells were collected and washed with phosphate-buffered saline (PBS) twice. Streptavidin magnetic beads (Thermo Fisher, USA) were placed in blocking buffer for 2h and put into every reaction to extract the biotin-coupled RNA compound. Tubes were placed in incubation while rotating at low speed (10rpm /min) for 4h. Beads were washed by lysis buffer five times. Then, Trizol reagent was utilized to retrieve the RNAs that interacted with miRNAs. Quantity of circFAM114A2 in bound portions was assessed by qRT-PCR and agarose gel electrophoresis.

Biotin-coupled probe pull down assay

Biotinylated probe was targeted to bind the junctional region of circFAM114A2. Oligo probe served as control. Approximately 1×10^7 cells were washed with pre-cooled PBS, and then lysed using lysis buffer. The lysed products were placed in incubation using 3 µg biotinylated probes at room temperature for 2h.

Then, cell lysates were incubated with 50 µl streptavidin magnetic beads for an additional 4h. The beads were cleaned using lysis buffer five times and miRNAs in the pull-down material were isolated utilizing Trizol reagent and assessed with qRT-PCR assay.

Agarose gel electrophoresis

The agarose gel was made of agarose powder, 1×TAE solution and nucleic acid dye. About 2 µl DNA ladder was added to 8 µL of the PCR product, and loaded to agarose gels. The constant-pressure 200 V was set up for 20 min electrophoresis. When electrophoresis ends, the gel was viewed by ultraviolet lamp to identify the region of DNA.

Northern blot

Northern blot was conducted using northern blot kit. In short, approximately 30 µg of total RNA was denatured by formaldehyde and ran under electrophoresis in a 1% agarose-formaldehyde gel. Electrophoresed RNAs were moved onto a Hybond-N+nylon membrane. The biotinlabeled DNA probes were used for hybridization with relative RNAs. Biotin chromogenic detection was utilized to identify the bound RNAs. Lastly, membranes were assessed by Image Lab software (Bio Rad, USA).

Fluorescence in situ hybridization (FISH)

Cy3-labeled probes specific to circFAM114A2 and fam-labeled probes specific to miR-222-3p/miR-146a-5p were constructed and produced through Genepharma (Shanghai, China) and probe signals were identified through a Fluorescent In Situ Hybridization Kit (Genepharma, Shanghai, China) as per established protocol. Pictures were attained on a Zeiss LSM880 NLO confocal microscope system (Leica Microsystems, Germany).

Luciferase reporter assay

HEK293 cells were co-transfected with mutant or wild 3'-UTR fragments of P27 or P21 and miRNA mimics utilizing Lipofectamine3000 (Invitrogen, CA) as per established instructions. After 24h post-transfection, firefly and renilla luciferase activities were quantified consistently by utilizing dual luciferase reporter assay system (Promega, USA). Lastly, the proportion of luminescence through luciferase was measured and every experiment was conducted three times.

Immunohistochemistry (IHC)

Paraffin-embedded tumors from mice were sliced to 4 µm slides. Tissue slides were rehydrated with different grade ethanol, and then placed in sodium citrate buffer (pH=6). Antigen was isolated utilizing heating through microwave. Slides were dipped in 3% H2O2 for 10 min and then treated with P27 or P21 antibody at 4°C overnight. After washed, the slides were incubated with HRP-conjugated antibody and standard avidin biotinylated peroxidase complex method. The images were viewed with a microscope.

The degree of positivity was assessed by at least two pathologists based on the proportion of positive tumor cells.

Xenografts in mice

Approximately 1×107 cells underwent a stable transfection using si circFAM114A2, si NC, circFAM114A2 and vector were inoculated into axilla of the BALB/C nude mice (4-6 weeks old, 18-22 g, 4 mice/group) subcutaneously. We divided nude mice inoculated with si circFAM114A2 and si NC transfected cells into four groups and named them si circFAM114A2+cisplatin group, si NC+cisplatin group, si circFAM114A2+saline group and si NC+saline group. One week after inoculation, nude mice in the experimental groups were intraperitoneally injected with cisplatin (5mg/kg) every three days, while the control groups were injected with the same volume of saline. Tumor evolution was followed each week, and the width (W) and length (L) were quantified utilizing calipers. The volume (V) of tumor was measured utilizing the formula $V= (W^2×L)/2$. After four weeks, the mice were sacrificed and tumor bulk was quantified. Animal experiments were conducted according to ethics guidelines for animal studies and granted approval through the animal ethics board of Nanjing Medical University.

Statistical analyses

Results were assessed utilizing SPSS version 22.0 and depicted as mean±standard deviation. The P value was statistically significant when less than 0.05. Two-tailed Student's t-test and one-way ANOVA was conducted to assess variation among the groups. Correlation was assessed through Pearson's correlation and Spearman's rank correlation test. Survival curves were imaged utilizing the Kaplan-Meier method, and variation was assessed through log-rank test.

Results

CircFAM114A2 was down-regulated in BCa and associated with prognosis of BCa patients

RNA sequencing on five pairs of BCa tissues was carried out and differentially expressed circRNAs were screened out by certain conditions (Additional Fig. 1A). The down-regulated circRNAs were sorted by fold change of more than 2 and P value of less than 0.05 and then screened them with an average read count of normal tissue more than 150. We found that circFAM114A2 was one of three most down-regulated circRNAs (Additional Fig. 1B). Among them, circFAM114A2 had a much higher tissue average read count than other two circRNAs. Then, we validated head-to-tail splicing through RT-PCR of circFAM114A2 using an estimated size established by Sanger sequencing (Fig. 1A). To study levels of circFAM114A2 in BCa tissue, levels of circFAM114A2 in 46 paired BCa and matched adjacent healthy bladder tissue were detected. Next, results showed that circFAM114A2 was significantly reduced in BCa tissues (Fig. 1B) and 8 BCa lines (BIU87, TCC, RT4, 5637, T24, J82, UMUC, and 253J) in comparison to SV-HUC, a healthy urothelial cell line (Fig. 1C). Additionally, we also found that FAM114A2 mRNA was down-regulated in

BCa tissue (Additional Fig. 2A) and cell lines (Additional Fig. 2B). Then, the convergent primers to increase FAM114A2 mRNA and divergent primers to amplify circFAM114A2 were designed. CircFAM114A2 could only be amplified by divergent primers in cDNA rather than gDNA (Fig. 1D). Through utilizing qRT-PCR, we additionally showed that FAM114A2 mRNA was drastically decreased post-RNase R addition, though circFAM114A2 was impervious to RNase R (Fig. 1E). Patients with different circFAM114A2 expression value were divided into low- and high- circFAM114A2 groups. The mean value was 0.000125103. And we found levels of circFAM114A2 were negatively associated with histological grade (P = 0.02), but not with the use of additional clinicopathological parameters, such as age, gender, tumor node metastasis stage (TNM) and tumor size (Table 1). We predicted recurrence and progression in NMIBC patients and stratificate the risk group by EORTC method (29). We found that recurrence scores were lower in high circFAM114A2 expression group (Table 1). In addition, BCa patients with higher circFAM114A2 levels had better overall survival (Fig. 1F). Taken together, these data indicate that circFAM114A2 was down-regulated in BCa and related to prognosis.

CircFAM114A2 inhibited the progression and enhanced the cisplatin chemosensitivity of BCa cells in vitro

To examine the role of circFAM114A2 in BCa, we separately chose a high malignant BCa cell line T24 and low malignant BCa cell line 5637, and conducted further functional assays. We transfected the circFAM114A2 overexpression vector and knock-down lentivirus into T24 and 5637 cells. We discovered that levels of circFAM114A2 were substantially changed while levels of FAM114A2 mRNA had no significant change (Fig. 2A,E). Furthermore, CCK-8 assays show that viability of T24 and 5637 cells was increased in the circFAM114A2 knockdown group in comparison to the controls (Fig. 2B), while viability was significantly reduced in the circFAM114A2-overexpression group in comparison to the vectors (Fig. 2F). The colony numbers of circFAM114A2 knockdown group were significantly increased (Fig. 2C), while the colony numbers of circFAM114A2 overexpression group was substantially decreased (Fig. 2G). In order to reveal the role of circFAM114A2 in cisplatin chemosensitivity, we designed 10 gradient cisplatin diluted concentration (0, 2, 4, 8, 16, 32, 40, 50, 64, 128 μmol/L). The cell viability curve of the cisplatin treatment assays for calculating the IC50 presented in the Additional Fig. 3. CCK-8 assay indicated that circFAM114A2 overexpression may drastically constrain growth of T24 and 5637s across different diluted concentrations of cisplatin compared to the vector group. In the circFAM114A2 knockdown group, proliferation of T24 and 5637 cells was significantly increased across the different diluted concentrations of cisplatin in comparison to the relative control group. The IC50 value of circFAM114A2 knockdown group was substantially higher than the controls (Fig. 2D). Furthermore, the IC50 of cisplatin to T24 and 5637 cells in the circFAM114A2 overexpression cohort was meaningfully reduced compared to the vector group (Fig. 2H). Additionally, apoptosis experiments indicate that circFAM114A2 induced cell apoptosis in BCa cells (Additional Fig. 4). Overexpression circFAM114A2 induced higher apoptosis rate compared to vector group with cisplatin treatment (Additional Fig. 4). All the data validated that circFAM114A2 could inhibit the progression and enhance the cisplatin chemosensitivity of BCa cells *in vitro*.

CircFAM114A2 acts as a molecular sponge for miR-222-3p and miR-146a-5p

Many studies have described that circRNAs can perform as miRNA sponges. They can bind relative functioning miRNAs and influence their levels. In order to investigate whether circFAM114A2 may function as a sponge for miRNAs in BCa cells, three publicly accessible predictive algorithms miRanda (http://www.microrna.org/microrna/home.do), regRNA (https://regrna.mbc.nctu.edu.tw/html/prediction.html) and RNAhybrid (https://bibiserv.cebitec.uni-bielefeld.de/rnahybrid/) were used to forecast the potential binding miRNAs of circFAM114A2. Overall, 10 potential miRNAs were predicted by the 3 prediction instruments (Fig. 3A). Subsequently, the biotin-labeled probe pull down tests were applied to examine where circFAM114A2 can bind these potential miRNAs. The biotin-labeled probe was confirmed to bring down circFAM114A2 in T24 cells (Fig. 3B,C). We detected expression of 10 potential miRNAs, and data indicated that only miR-222-3p and miR-146a-5p were abundantly pulled down by circFAM114A2 (Fig. 3D). To additionally verify the sponge effect of circFAM114A2, we administered biotin-labeled miR-222-3p and miR-146a-5p mimics to confirm the direct binding of these miRNAs to circFAM114A2. As data indicates, biotin-labeled miR-222-3p/miR-146a-5p mimics detained additional circFAM114A2 compared to the biotin-labeled negative control (Fig. 3E,F). We examined the level of miR-222-3p/miR-146a-5p in T24 and 5637 BCa cells which had different expression level of circFAM114A2. The results showed that the expression of miR-222-3p and miR-146a-5p were increase by circFAM114A2 knockdown (Fig. 3G, I), while overexpression circFAM114A2 reduced the miR-222-3p and miR-146a-5p expression (Fig. 3H, J). Furthermore, RNA FISH experiments indicated that circFAM114A2 and miR-222-3p/miR-146a-5p co-localized in the cytoplasm and nucleus (Fig. 3K,L). Overall, results prove that circFAM114A2 can bind to both miR-222-3p and miR-146a-5p.

MIR-222-3p/146a-5p interference rescued the progression inhibition and cisplatin chemo-sensitization induced by circFAM114A2 in BCa cells

We found that miR-222-3p and miR-146a-5p had high expression in 46 BCa tissues in comparison to surrounding healthy tissues (Fig. 4A). A negative relationship among levels of circFAM114A2 and miR-222-3p/miR-146a-5p was indicated utilizing Pearson correlation analysis (Fig. 4B). Due to the interaction of circFAM114A2 and miR-222-3p/miR-146a-5p, the potential function of miR-222-3p and miR-146a-5p in BCa cells were studied by transfecting miRNA and NC mimics. Overexpression of miR-222-3p or miR-146a-5p substantially encouraged the proliferation of T24 and 5637 cells (Fig. 4C). In addition, the IC50 values of cells transfected with miR-222-3p or miR-146a-5p mimics were substantially increased in comparison to NC mimic group across both T24 and 5637 cells. (Fig. 4D). The rescue experiment was performed by co-transfecting circFAM114A2 and miR-222-3p/miR-146a-5p mimics into BCa cells. CCK-8 and colony formation assay indicated that high expression of circFAM114A2 was associated with an inhibition in growth. However, this influence may, in part, be inhibited by ectopic miR-222-3p or miR-146a-5p expression (Fig. 4E,G). More than that, results from the CCK-8 assay suggested that progression of BCa cell growth was appreciably hindered when treated with different diluted concentrations of cisplatin by overexpression of circFAM114A2, while the ectopic expression of miR-222-3p or miR-146a-5p could partly attenuate this phenomenon (Fig. 4F). All these data confirm that miR-222-3p/146a-5p could rescue the inhibition of progression and cisplatin chemosensitization induced by circFAM114A2 in BCa cells.

Mir-222-3p/mir-146a-5p Rescued Cell Cycle Arrest Induced By Circfam114a2

Flow cytometry results indicated that less cells were dispersed in the G1 phase of circFAM114A2 knockdown group (Fig. 5A-D), while more cells were dispersed in G1 phase of circFAM114A2 overexpression group (Fig. 5I-L), which implied that circFAM114A2 likely stimulated G1/S cell cycle arrest. However, more cells were dispersed in S phase in miR-222-3p/miR-146a-5p mimics groups compared with control groups (Fig. 5E-H). Transfection of miR-222-3p/miR-146a-5p mimics in circFAM114A2 overexpression cells could rescue G1/S cell cycle arrest phenomenon induced by circFAM114A2 (Fig. 5I-L).

CircFAM114A2 influences the expression of P27 and P21 through sponging miR-222-3p and miR-146a-5p

In three pairs of circFAM114A2 overexpression and negative control cells, mRNA sequencing and enrichment analysis (GSEA analysis) was performed (Additional Fig. 5). We found that the cell-cycle transition genes, P27 and P21, were significantly related to circFAM114A2 expression. Hence, we selected P27 and P21 from the results for additional validation. According to miRanda and TargetScan prediction, we determined that miR-222-3p and miR-146a-5p target the 3'-UTR of P27 and P21, respectively (Fig. 6A). Dual luciferase reporter assay was also carried out to confirm miR-222-3p/miR-146a-5p binding with P27/P21. The wild-type and mutant 3'-UTR of P27 and P21 was added to the construct reporter plasmids, respectively. Co-transfection of miR-222-3p mimic and wild-type P27 reporter plasmid reduced luciferase activity dramatically. Co-transfection of miR-146a-5p and wild type P21 reporter plasmid also reduced luciferase activity. (Fig. 6B). Quite the reverse, co-transfection of miR-222-3p or miR-146a-5p mimics and mutated P27 or P21 vectors indicated no significant influence on luciferase activity (Fig. 6B). The qRT-PCR and western blot results revealed that miR-222-3p/miR-146a-5p could reduce the expression of P27/P21 respectively (Fig. 6C,D). We also preformed qRT-PCR and western blot experiments to validate if miR-222-3p could influence the expression of P21 and miR-146a-5p could influence the expression of P27 (Additional Fig. 6). The results showed that these two pathways were two separate pathways. The qRT-PCR and western blot results indicated that knockdown of circFAM114A2 could decrease P27 and P21 mRNA and protein (Fig. 6E,F). Consequently, high levels of circFAM114A2 may heighten mRNA and protein expression of P27 and P21 (Fig. 6G-J). On the other hand, co-transfection of miR-222-3p or miR-146a-5p mimics and circFAM114A2 partly inhibited the increased expression of P27 and P21 induced by circFAM114A2 (Fig. 6G-J). All these findings confirmed that P27 and P21 were directly regulated by miR-222-3p and miR-146a-5p respectively. Overall, results indicated that circFAM114A2 inhibited BCa advancement and cisplatin chemo-resistance by eliminating miR-222-3p and miR-146a-5p oncogenic effect. In this study, we revealed two axes of circFAM114A2-miR-222-3p-P27 and circFAM114A2-miR-146a-5p-P21 which played an important role in inhibition of BCa progression and cisplatin chemo-resistance.

CircFAM114A2 inhibited growth of xenografted tumor in vivo

To examine if high levels of circFAM114A2 affect tumor growth *in vivo*, T24 cells transfected using circFAM114A2 or vector were inoculated in nude mice subcutaneously. After four weeks, we observed the tumor in nude mice and removed it (Fig. 7A-B). CircFAM114A2 overexpression group had a significantly lower average tumor weight (Fig. 7C) and lower mean tumor volume (Fig. 7D) than those of vector group. IHC assessment showed that P27 and P21 levels were promoted by overexpression circFAM114A2 (Fig. 7E). QRT-PCR results showed miR-222-3p and miR-146a-5p expression levels were reduced in 4 pairs of xenograft tumors transfected with circFAM114A2 compared with those of NC group (Fig. 7F-G). Western blot results also showed that P27 and P21 expression level were increased in circFAM114A2 overexpression group (Fig. 7H).

CircFAM114A2 promoted cisplatin sensitivity in vivo

To investigate whether circFAM114A2 could influence the sensitivity of cisplatin chemotherapy *in vivo*, T24 cells transfected with si circFAM114A2 or si NC were inoculated in nude mice subcutaneously. One week after inoculation, nude mice in the experimental groups were intraperitoneally injected with cisplatin (5 mg/kg) every three days, while the control groups were injected with the same volume of saline. After four weeks, we observed the tumor in nude mice and removed it (Fig. 8A-B). The volume and weight of tumors in cisplatin treated group were lower than those in saline control group (Fig. 8C-D). The tumor weight and volume of si circFAM114A2 group treated with cisplatin were higher compared si NC group treated with cisplatin (Fig. 8C-D). All the results indicated that circFAM114A2 could promote cisplatin sensitivity *in vivo*.

Discussion

During recent years, circRNAs have been increasingly shown to act as vital factors in the incidence and formation of BCa (17, 18, 20). We detected circFAM114A2 through circRNA sequencing technology and confirmed that circFAM114A2 was decreased in BCa tissues and cell lines consistent with a study by Liu *et al.* (30). BCa patients with lower circFAM114A2 levels had shortened survival. Subsequently, we found that circFAM114A2 inhibited progression of BCa and encouraged sensitivity of BCa cells to cisplatin *in vitro* and *vivo*. CircFAM114A2 may directly associate with miR-222-3p/miR-146a-5p, and then perform as a miRNA sponge to control levels of miR-222-3p/miR-146a-5p target gene P27/P21, which suppressed progression of BCa. Overall, this data showed that circFAM114A2 performed as a tumor-suppressor in BCa. It is very interesting that the screening of downstream miRNAs of circFAM114A2 in our paper was different from those reported by Liu et al [30]. The differences may be caused by the different selection of prediction databases and the different screening conditions in each database. Except MiRanda and RNAhybrid database, regRNA was also used in our prediction process. The screening conditions like combined score or minimum free energy may also different in these two papers. For the selection of downstream mRNA, mRNA sequencing was performed in circFAM114A2 overexpression and negative control cells. Then target genes P27 and P21 were identified through enrichment analysis. While Liu et al. predicted and selected the downstream target mRNA by using publicly available databases [30].

CircRNAs may perform as miRNA sponges to carry out their function. Yang *et al.* showed that circITCH can inhibit the progression of BCa through circITCH/miR-17 or miR-224/P21 or PTEN pathway (17). While some circRNAs can influence the modulation of transcription, some circRNAs can be translated (31). CircRNAs are playing an increasingly important role in the treatment of tumors. For example, circRNAs can regulate immune function and affect the occurrence and development of tumors, which provides more enlightenment for immunotherapy of different tumors (32). CircMET can lead to immunosuppression and resistance to anti-PD1 therapy in hepatocellular carcinoma (33). In addition, some studies have found that circRNA can enrich in exosomes and further affect the occurrence and development of tumors (26). Studies have shown that detection of circRNA in serum exosomes can distinguish cancer patients from healthy controls, and circRNA in exosomes can be used as a biomarker for liquid biopsy (34). In our study, we identified that circFAM114A2 was generally down-regulated in BCa tissues through circRNA sequencing technology. We further confirmed that circFAM114A2 was decreased in BCa tissues and cell lines by qRT-PCR. Afterward, we found that circFAM114A2 inhibited the proliferation of BCa and encouraged the sensitivity of BCa cells *in vitro* and in *vivo* through the CCK-8 assay, clone formation assay, IC50 determination and xenografts. Then, by RNA pull down assay and RNA FISH, we found that circFAM114A2 may sponge miR-222-3p and miR-146a-5p. Next, by luciferase reporter assay, we discovered that miR-222-3p and miR-146a-5p can be bound to P27 and P21, respectively. The rescue experiments confirmed that circFAM114A2 inhibited BCa proliferation and increased cisplatin sensitivity by circFAM114A2-miR-222-3p-P27 and circFAM114A2-miR-146a-5p-P21 axes. We also explored the relationship between these two pathways. And the results of qRT-PCR and western blot showed that these two pathways are more inclined to two independent pathways. However, P27 and P21 play a synergistic role in promoting cell cycle arrest (35). And they are consistent in inhibiting tumor proliferation and promoting cisplatin chemotherapy sensitivity in bladder cancer (36). So we think that these two pathways are independent in mechanism but synergistic in inhibiting tumor development. However, circRNAs can also promote the progression of cancer. For instance, circTP63 could promote progression of lung squamous cell carcinoma via up-regulating FOXM1 expression (37). Advanced RNA sequencing (RNA-seq) and bioinformatics technologies have helped us to identify various circRNAs and reveal their important functions. With more attention and research, the biological functions of circRNAs have been brought to light.

Cisplatin has always had a vital function in the chemotherapy of BCa. The long-term survival of patients is greatly hindered due to cisplatin resistance (38). Therefore, there is a need for more attention to reveal mechanisms of cisplatin resistance. Previously, Yuan et al. reported that circCDR1as could improve the sensitivity of BCa to cisplatin through increasing APAF1 levels by inhibiting miR-1270 (20). Our research also revealed a chemo-sensitization function of circFAM114A2 in BCa treatment. CCK-8 assay indicated that circFAM114A2 could drastically block the growth of BCa cells across different diluted concentrations of cisplatin. In the circFAM114A2 knockdown group, the IC50 was higher than the relative control group. On the other hand, in the circFAM114A2 overexpression group, the IC50 was lower when compared with relative control group. During the BCa cell lines verification, we found that cell lines (TCC, T24 and 253J) which had very low expression of circFAM114A2 are all relative high malignant degree BCa cell lines and

had mutations in different oncogenes like P53, H-ras or TREK2. So these cell lines may intrinsic resistant to chemotherapy because of high malignant degree or relative oncogene mutation. There are indeed some mutations in oncogenes like P53, H-ras or TREK2. But we did not find any association between these mutation oncogenes and expression of circFAM114A2. It is need to do more research on this area in the future. As reported, cell cycle regulation and cell apoptosis are the theoretical basis of cisplatin action and play important roles in cisplatin chemotherapy resistance (21, 22). It has been reported that tumors are most sensitive to cisplatin in G1 phase (39, 40). Therefore, blocking tumor cells in the G1 phase can enhance their sensitivity to cisplatin. In our study, we found that high expression of circFAM114A2 could block more BCa cells in the G1 phase. Furthermore, we discovered that high expression of circFAM114A2 may heighten the apoptosis rate of BCa cells. Many studies have shown that circRNAs can influence the apoptosis level of gastric cancer, urothelial carcinoma and non-small cell lung cancer cells (41–43). Hence, our results suggest that improved sensitivity induced by circFAM114A2 may also relate to a high apoptosis rate.

Conclusions

Based on our data, we confirmed that circFAM114A2 was decreased in BCa tissue and cell lines. Furthermore, patients with higher circFAM114A2 levels had better overall survival. CircFAM114A2 can inhibit the proliferation of BCa cells, block cells in G1 phase, induce cell apoptosis and increase the sensitivity to cisplatin through sponging miR-146a-5p/miR-222-3p and controlling P21 and P27 expression levels. In summary, circFAM114A2 potentially have a function in predicting cisplatin chemosensitivity in BCa patients and may be a new possible biomarker and treatment target for BCa.

Abbreviations

CircRNA: circular RNA; miRNA: micro RNA; ncRNA: non-coding RNA; BCa: Bladder cancer; MIBC: muscle invasive bladder cancer; NMIBC: non-muscle invasive bladder cancer; FISH: Fluorescence In Situ Hybridization

Declarations

Ethics approval and consent to participate:

Participants were asked to sign informed consent before using clinical resources. Animal experiments were conducted according to ethics guidelines for animal studies and granted approval through the animal ethics board of Nanjing Medical University.

Consent for publication:

Not applicable.

Availability of data and materials:

All data generated or analyzed during this study are included either in this article or in the supplementary information files.

Authors' contributions:

QL and HY conceived and designed the study. JL, ZZ, JW, HY, JH, DF, BY, QW and PL performed the experiments. JL and XY wrote the paper. QL and HY reviewed and edited the manuscript. All authors read and approved the manuscript.

Funding:

This work was supported by the National Natural Science Foundation of China (No. 81772711; 81602235; 82072832), Jiangsu Province's Key Provincial Talents Program (ZDRCA2016006)the "333" project of Jiangsu Province (LGY2016002 and 2018055), the Provincial Initiative Program for Excellency Disciplines of Jiangsu Province (No. BE2016791), and the Priority Academic Program Development of Jiangsu Higher Education Institutions (PAPD).

Conflicts of interest:

The authors declare that they have no competing interests.

Acknowledgements

Not applicable

References

1. Antoni S, Ferlay J, Soerjomataram I, Znaor A, Jemal A, Bray F. Bladder Cancer Incidence and Mortality: A Global Overview and Recent Trends. Eur Urol. 2017;71(1):96–108.
2. van Rhijn BW, Burger M, Lotan Y, Solsona E, Stief CG, Sylvester RJ, et al. Recurrence and progression of disease in non-muscle-invasive bladder cancer: from epidemiology to treatment strategy. Eur Urol. 2009;56(3):430–42.
3. Dy GW, Gore JL, Forouzanfar MH, Naghavi M, Fitzmaurice C. Global Burden of Urologic Cancers, 1990–2013. Eur Urol. 2017;71(3):437–46.
4. Alfred Witjes J, Lebret T, Comperat EM, Cowan NC, De Santis M, Bruins HM, et al. Updated 2016 EAU Guidelines on Muscle-invasive and Metastatic Bladder Cancer. Eur Urol. 2017;71(3):462–75.
5. Sagalowsky AI. Words of Wisdom: re: a systematic review of neoadjuvant and adjuvant chemotherapy for muscle-invasive bladder cancer. Eur Urol. 2013;63(3):579–80.
6. Memczak S, Jens M, Elefsinioti A, Torti F, Krueger J, Rybak A, et al. Circular RNAs are a large class of animal RNAs with regulatory potency. Nature. 2013;495(7441):333–8.
7. Dong Y, He D, Peng Z, Peng W, Shi W, Wang J, et al. Circular RNAs in cancer: an emerging key player. J Hematol Oncol. 2017;10(1):2.

8. Zhang XO, Dong R, Zhang Y, Zhang JL, Luo Z, Zhang J, et al. Diverse alternative back-splicing and alternative splicing landscape of circular RNAs. Genome Res. 2016;26(9):1277–87.
9. Cheng Y, Sun H, Wang H, Jiang W, Tang W, Lu C, et al. Star Circular RNAs In Human Cancer: Progress And Perspectives. Onco Targets Ther. 2019;12:8249–61.
10. Bach DH, Lee SK, Sood AK. Circular RNAs in Cancer. Mol Ther Nucleic Acids. 2019;16:118–29.
11. Kristensen LS, Hansen TB, Veno MT, Kjems J. Circular RNAs in cancer: opportunities and challenges in the field. Oncogene. 2018;37(5):555–65.
12. Hansen TB, Jensen TI, Clausen BH, Bramsen JB, Finsen B, Damgaard CK, et al. Natural RNA circles function as efficient microRNA sponges. Nature. 2013;495(7441):384–8.
13. Gebert LFR, MacRae IJ. Regulation of microRNA function in animals. Nature reviews Molecular cell biology. 2019;20(1):21–37.
14. Catto JW, Alcaraz A, Bjartell AS, De Vere White R, Evans CP, Fussel S, et al. MicroRNA in prostate, bladder, and kidney cancer: a systematic review. Eur Urol. 2011;59(5):671–81.
15. Li Q, Wang H, Peng H, Huang Q, Huyan T, Huang Q, et al. MicroRNAs: Key Players in Bladder Cancer. Mol Diagn Ther. 2019;23(5):579–601.
16. Hansen TB, Kjems J, Damgaard CK. Circular RNA and miR-7 in cancer. Cancer Res. 2013;73(18):5609–12.
17. Yang C, Yuan W, Yang X, Li P, Wang J, Han J, et al. Circular RNA circ-ITCH inhibits bladder cancer progression by sponging miR-17/miR-224 and regulating p21, PTEN expression. Mol Cancer. 2018;17(1):19.
18. Lu Q, Liu T, Feng H, Yang R, Zhao X, Chen W, et al. Circular RNA circSLC8A1 acts as a sponge of miR-130b/miR-494 in suppressing bladder cancer progression via regulating PTEN. Mol Cancer. 2019;18(1):111.
19. Yang X, Yuan W, Tao J, Li P, Yang C, Deng X, et al. Identification of circular RNA signature in bladder cancer. J Cancer. 2017;8(17):3456–63.
20. Yuan W, Zhou R, Wang J, Han J, Yang X, Yu H, et al. Circular RNA Cdr1as sensitizes bladder cancer to cisplatin by upregulating APAF1 expression through miR-1270 inhibition. Mol Oncol. 2019;13(7):1559–76.
21. Borst P, Jonkers J, Rottenberg S. What. Makes Tumors Multidrug Resistant? Cell Cycle. 2014;6(22):2782–7.
22. D W, SJ L. Cellular processing of platinum anticancer drugs. Nature reviews Drug discovery. 2005;4(4):307–20.
23. Pines J. p21 inhibits cyclin shock. Nature. 1994;369(6481):520–1.
24. Toyoshima H, Hunter T. p27, a novel inhibitor of G1 cyclin-Cdk protein kinase activity, is related to p21. Cell. 1994;78(1):67–74.
25. Ripani P, Delp J, Bode K, Delgado ME, Dietrich L, Betzler VM, et al. Thiazolides promote G1 cell cycle arrest in colorectal cancer cells by targeting the mitochondrial respiratory chain. Oncogene. 2019.

26. Wang C, Hamacher A, Petzsch P, Kohrer K, Niegisch G, Hoffmann MJ, et al. Combination of Decitabine and Entinostat Synergistically Inhibits Urothelial Bladder Cancer Cells via Activation of FoxO1. Cancers. 2020;12(2).
27. Cheng Y, Yang X, Deng X, Zhang X, Li P, Tao J, et al. MicroRNA-218 inhibits bladder cancer cell proliferation, migration, and invasion by targeting BMI-1. Tumour Biol. 2015;36(10):8015–23.
28. Tao J, Lu Q, Wu D, Li P, Xu B, Qing W, et al. microRNA-21 modulates cell proliferation and sensitivity to doxorubicin in bladder cancer cells. Oncol Rep. 2011;25(6):1721–9.
29. Sylvester RJ, van der Meijden AP, Oosterlinck W, Witjes JA, Bouffioux C, Denis L, et al. Predicting recurrence and progression in individual patients with stage Ta T1 bladder cancer using EORTC risk tables: a combined analysis of 2596 patients from seven EORTC trials. Eur Urol. 2006;49(3):466–5. discussion 75 – 7.
30. Liu T, Lu Q, Liu J, Xie S, Feng B, Zhu W, et al. Circular RNA FAM114A2 suppresses progression of bladder cancer via regulating ΔNP63 by sponging miR-762. Cell Death & Disease. 2020;11(1).
31. Jamal M, Song T, Chen B, Faisal M, Hong Z, Xie T, et al. Recent Progress on Circular RNA Research in Acute Myeloid Leukemia. Front Oncol. 2019;9:1108.
32. Zhang PF, Gao C, Huang XY, Lu JC, Guo XJ, Shi GM, et al. Cancer cell-derived exosomal circUHRF1 induces natural killer cell exhaustion and may cause resistance to anti-PD1 therapy in hepatocellular carcinoma. Mol Cancer. 2020;19(1):110.
33. Huang XY, Zhang PF, Wei CY, Peng R, Lu JC, Gao C, et al. Circular RNA circMET drives immunosuppression and anti-PD1 therapy resistance in hepatocellular carcinoma via the miR-30-5p/snail/DPP4 axis. Mol Cancer. 2020;19(1):92.
34. Zhu M, Liu X, Li W, Wang L. Exosomes derived from mmu_circ_0000623-modified ADSCs prevent liver fibrosis via activating autophagy. Hum Exp Toxicol. 2020:960327120931152.
35. Yoon M, Mitrea D, Ou L, Kriwacki RJBSt. Cell cycle regulation by the intrinsically disordered proteins p21 and p27. 2012;40(5):981–8.
36. Taguchi T, Kato Y, Baba Y, Nishimura G, Tanigaki Y, Horiuchi C, et al. Protein levels of p21, p27, cyclin E and Bax predict sensitivity to cisplatin and paclitaxel in head and neck squamous cell carcinomas. 2004;11(2):421–6.
37. Cheng Z, Yu C, Cui S, Wang H, Jin H, Wang C, et al. circTP63 functions as a ceRNA to promote lung squamous cell carcinoma progression by upregulating FOXM1. Nat Commun. 2019;10(1):3200.
38. Godwin JL, Hoffman-Censits J, Plimack E. Recent developments in the treatment of advanced bladder cancer. Urol Oncol. 2018;36(3):109–14.
39. Karen LD, Gay LG, Alan FW. Cytotoxicity of the anticancer agents cisplatin and taxol during cell proliferation and the cell cycle. Int J Cancer. 1994;57:847–55.
40. Manish AS, Gary KS. Cell cycle-mediated drug resistance: An emerging concept in cancer therapy. Clin Cancer Res. 2001;7:2168–81.

41. Chen Z, Ju H, Zhao T, Yu S, Li P, Jia J, et al. hsa_circ_0092306 Targeting miR-197-3p Promotes Gastric Cancer Development by Regulating PRKCB in MKN-45 Cells. Mol Ther Nucleic Acids. 2019;18:617–26.
42. Wang C, Tao W, Ni S, Chen Q. Circular RNA circ-Foxo3 induced cell apoptosis in urothelial carcinoma via interaction with miR-191-5p. OncoTargets therapy. 2019;12:8085–94.
43. Wang M, Shi J, Jiang H, Xu K, Huang Z. Circ_0014130 Participates in the Proliferation and Apoptosis of Nonsmall Cell Lung Cancer Cells via miR-142-5p/IGF-1 Axis. Cancer Biother Radiopharm. 2020.

Tables

Table 1 Correlations between the expression of circFAM114A2 and clinicopathological features in BCa patients.

Characteristics	Case	circ-FAM114A2		P value
		Low	High	
All cases	46	28	18	
Age(years)				0.152
<65	20	12	4	
≥65	26	16	14	
Gender				0.834
Male	34	21	13	
Female	12	7	5	
TNM stage				0.113
pTa-pT1	12	5	7	
pT2-pT4	34	23	11	
NMIBC/MIBC				0.113
NMIBC	12	5	7	
MIBC	34	23	11	
Histological grade				0.020*
Low	10	3	7	
High	36	25	11	
Histological grade				0.043*
G1	2	0	2	
G2	10	4	6	
G3	34	24	10	
Tumor size(cm)				0.080
<3	16	7	9	
≥3	30	21	9	
Recurrence score				0.023*
0	0	0	0	
1-4	0	0	0	
5-9	7	1	6	

10-17	5	4	1	
Progression score				0.424
0	0	0	0	
2-6	2	0	2	
7-13	4	2	2	
14-23	6	3	3	

*P<0.05

Figures

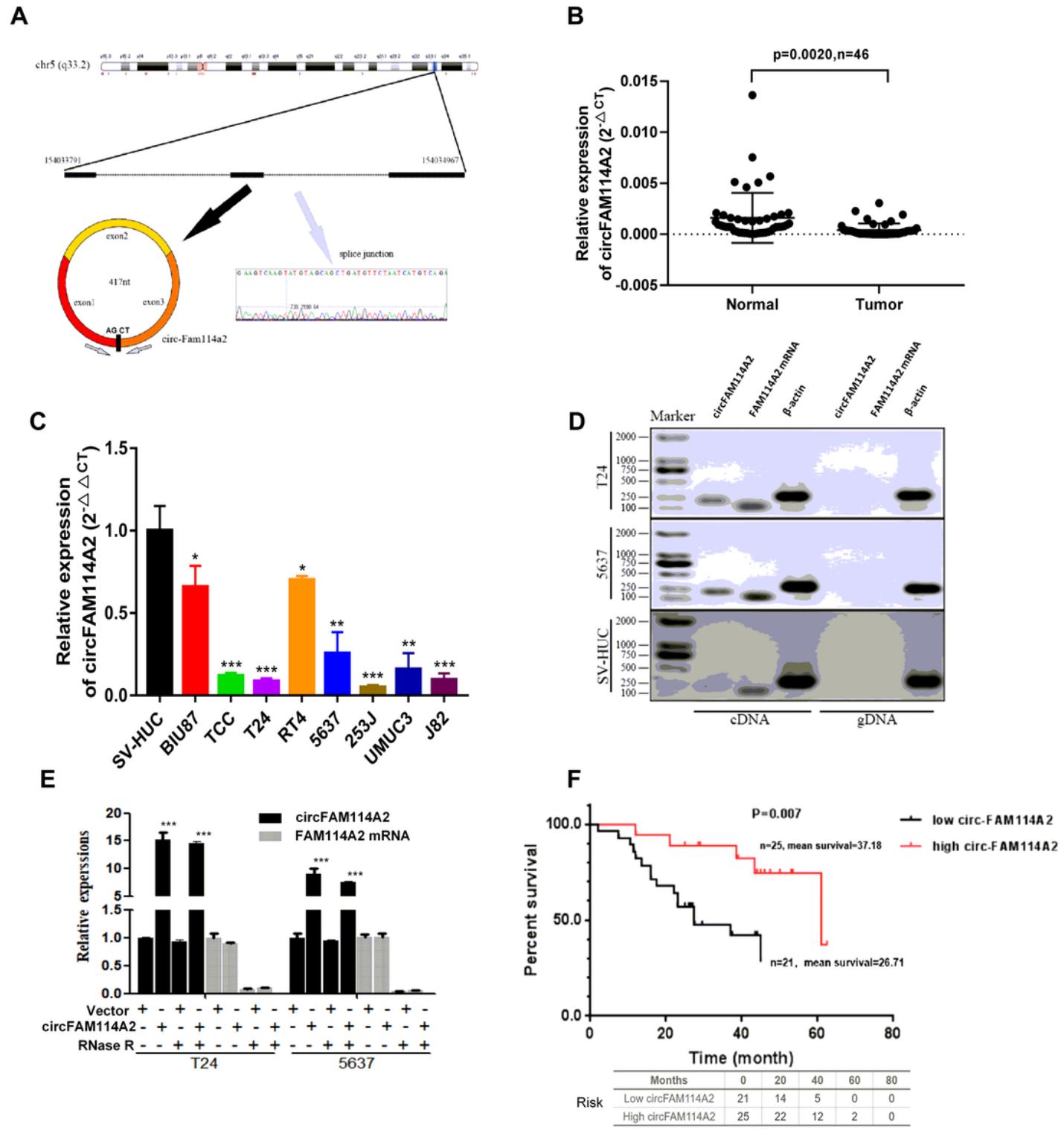

Figure 1

CircFAM114A2 was down-regulated in BCa tissues and cell lines and correlated with prognosis of patients. A Schematic illustration showed the circularization of FAM114A2 exon 1, exon2 and exon 3 forming circFAM114A2. The existence of circFAM114A2 was proved by RT-PCR and back splicing junction was verified by Sanger sequencing. Gray arrow indicates the special splicing junction of circFAM114A2. B QRT-PCR assay with divergent primers confirmed the low expression of circFAM114A2

in 46 pairs of human BCa tissues compared with their adjacent normal tissues. C The expression of circFAM114A2 in SV-HUC and BCa cell lines were measured by qRT-PCR (*P<0.05, **P<0.01,***P<0.001, Student's t-test). D The existence of circFAM114A2 was validated in sv-huc, 5637 and T24 cell lines by RT-PCR. Divergent primers amplified circFAM114A2 in cDNA but not genomic DNA (gDNA). β-actin was used as negative control. E The expression of circFAM114A2 and FAM114A2 mRNA in T24 and 5637 cells treated with or without RNase R were detected by qRT-PCR (***P<0.001, Student's t-test). F Kaplan-Meier plotter analysis of the correlation of circFAM114A2 expression level with overall survival of BCa patients. Data are mean±SD, n=3

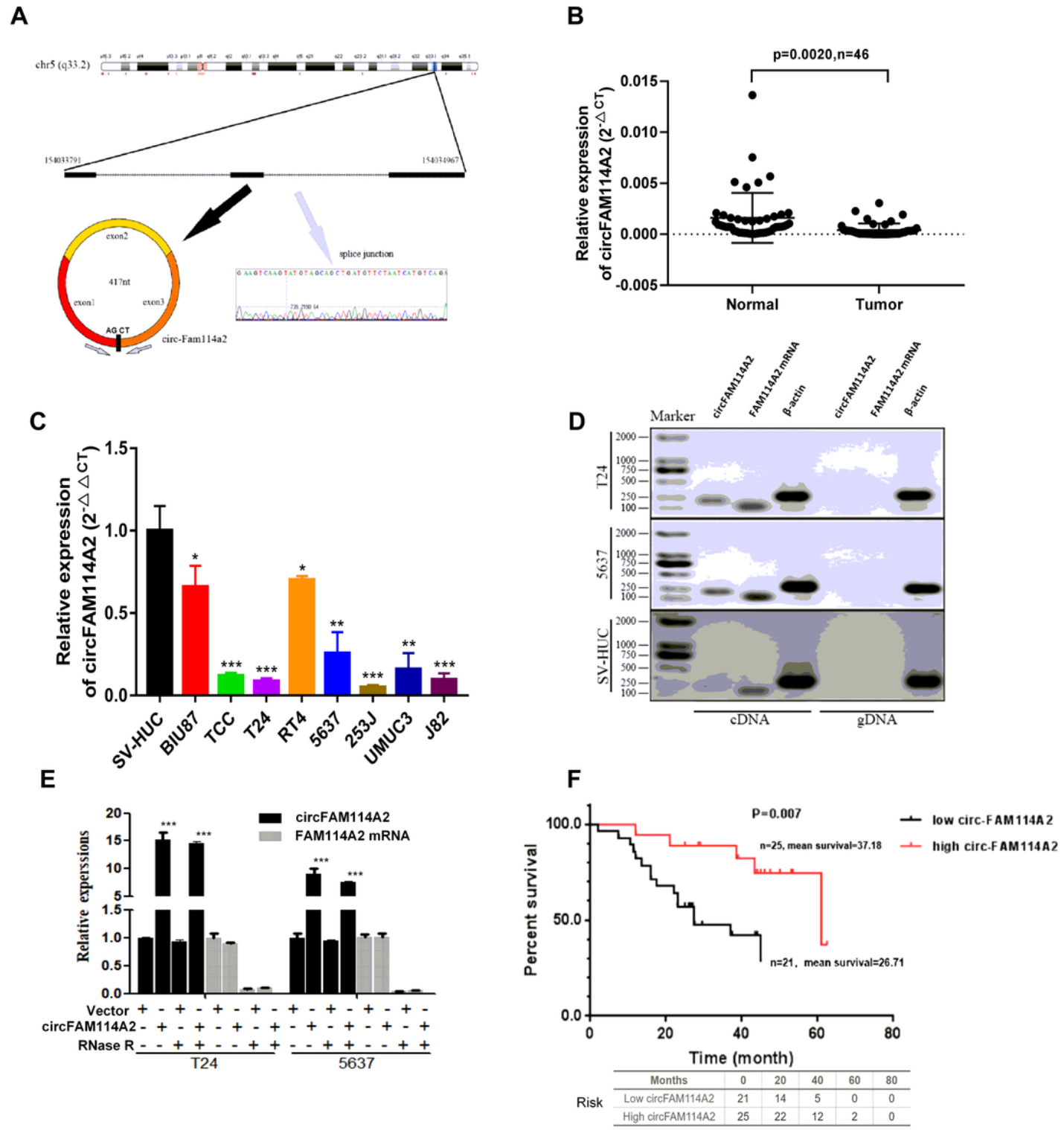

Figure 1

CircFAM114A2 was down-regulated in BCa tissues and cell lines and correlated with prognosis of patients. A Schematic illustration showed the circularization of FAM114A2 exon 1, exon2 and exon 3 forming circFAM114A2. The existence of circFAM114A2 was proved by RT-PCR and back splicing junction was verified by Sanger sequencing. Gray arrow indicates the special splicing junction of circFAM114A2. B QRT-PCR assay with divergent primers confirmed the low expression of circFAM114A2

in 46 pairs of human BCa tissues compared with their adjacent normal tissues. C The expression of circFAM114A2 in SV-HUC and BCa cell lines were measured by qRT-PCR (*P<0.05, **P<0.01,***P<0.001, Student's t-test). D The existence of circFAM114A2 was validated in sv-huc, 5637 and T24 cell lines by RT-PCR. Divergent primers amplified circFAM114A2 in cDNA but not genomic DNA (gDNA). β-actin was used as negative control. E The expression of circFAM114A2 and FAM114A2 mRNA in T24 and 5637 cells treated with or without RNase R were detected by qRT-PCR (***P<0.001, Student's t-test). F Kaplan-Meier plotter analysis of the correlation of circFAM114A2 expression level with overall survival of BCa patients. Data are mean±SD, n=3

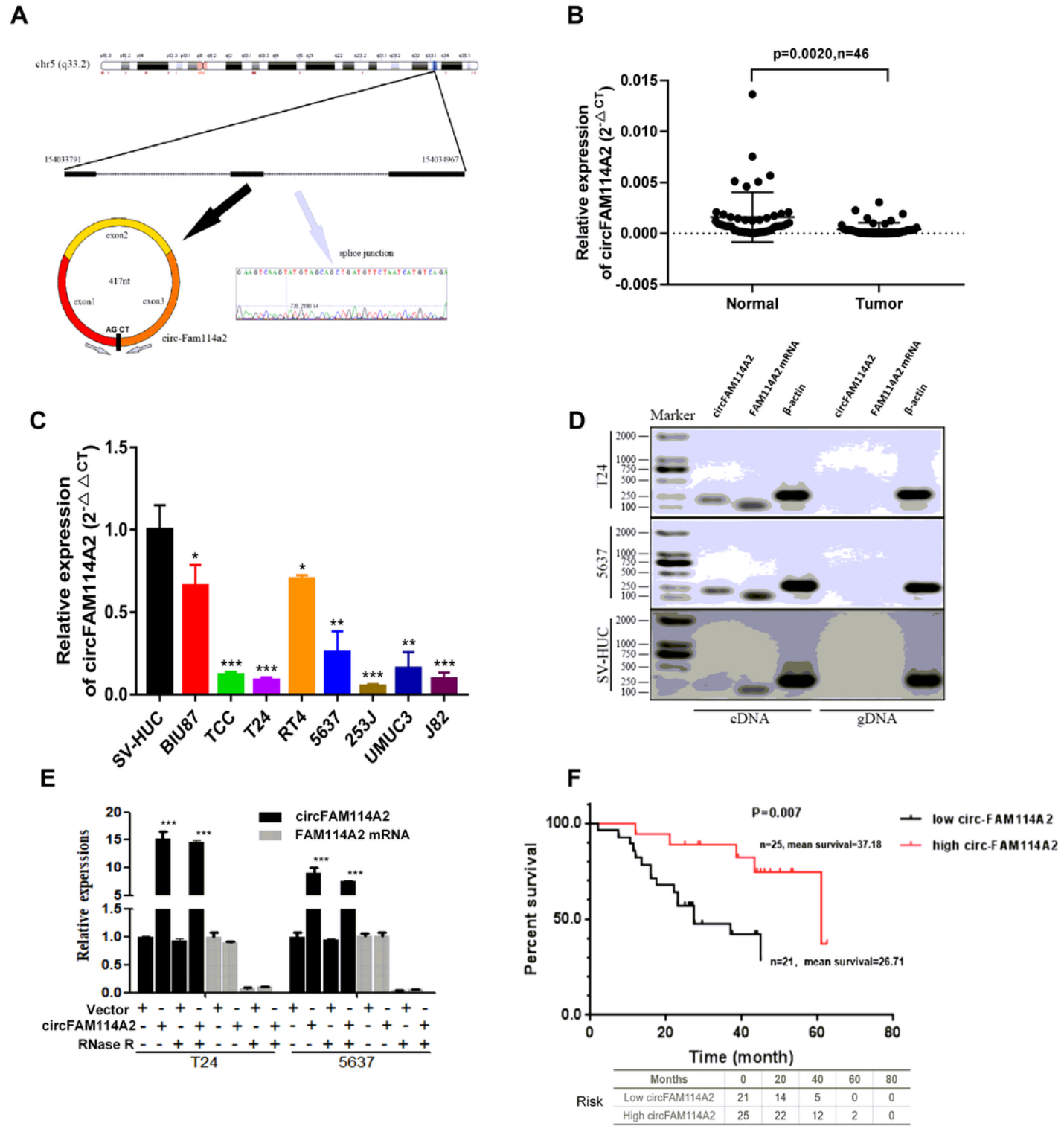

Figure 1

CircFAM114A2 was down-regulated in BCa tissues and cell lines and correlated with prognosis of patients. A Schematic illustration showed the circularization of FAM114A2 exon 1, exon2 and exon 3 forming circFAM114A2. The existence of circFAM114A2 was proved by RT-PCR and back splicing junction was verified by Sanger sequencing. Gray arrow indicates the special splicing junction of circFAM114A2. B QRT-PCR assay with divergent primers confirmed the low expression of circFAM114A2

in 46 pairs of human BCa tissues compared with their adjacent normal tissues. C The expression of circFAM114A2 in SV-HUC and BCa cell lines were measured by qRT-PCR (*P<0.05, **P<0.01,***P<0.001, Student's t-test). D The existence of circFAM114A2 was validated in sv-huc, 5637 and T24 cell lines by RT-PCR. Divergent primers amplified circFAM114A2 in cDNA but not genomic DNA (gDNA). β-actin was used as negative control. E The expression of circFAM114A2 and FAM114A2 mRNA in T24 and 5637 cells treated with or without RNase R were detected by qRT-PCR (***P<0.001, Student's t-test). F Kaplan-Meier plotter analysis of the correlation of circFAM114A2 expression level with overall survival of BCa patients. Data are mean±SD, n=3

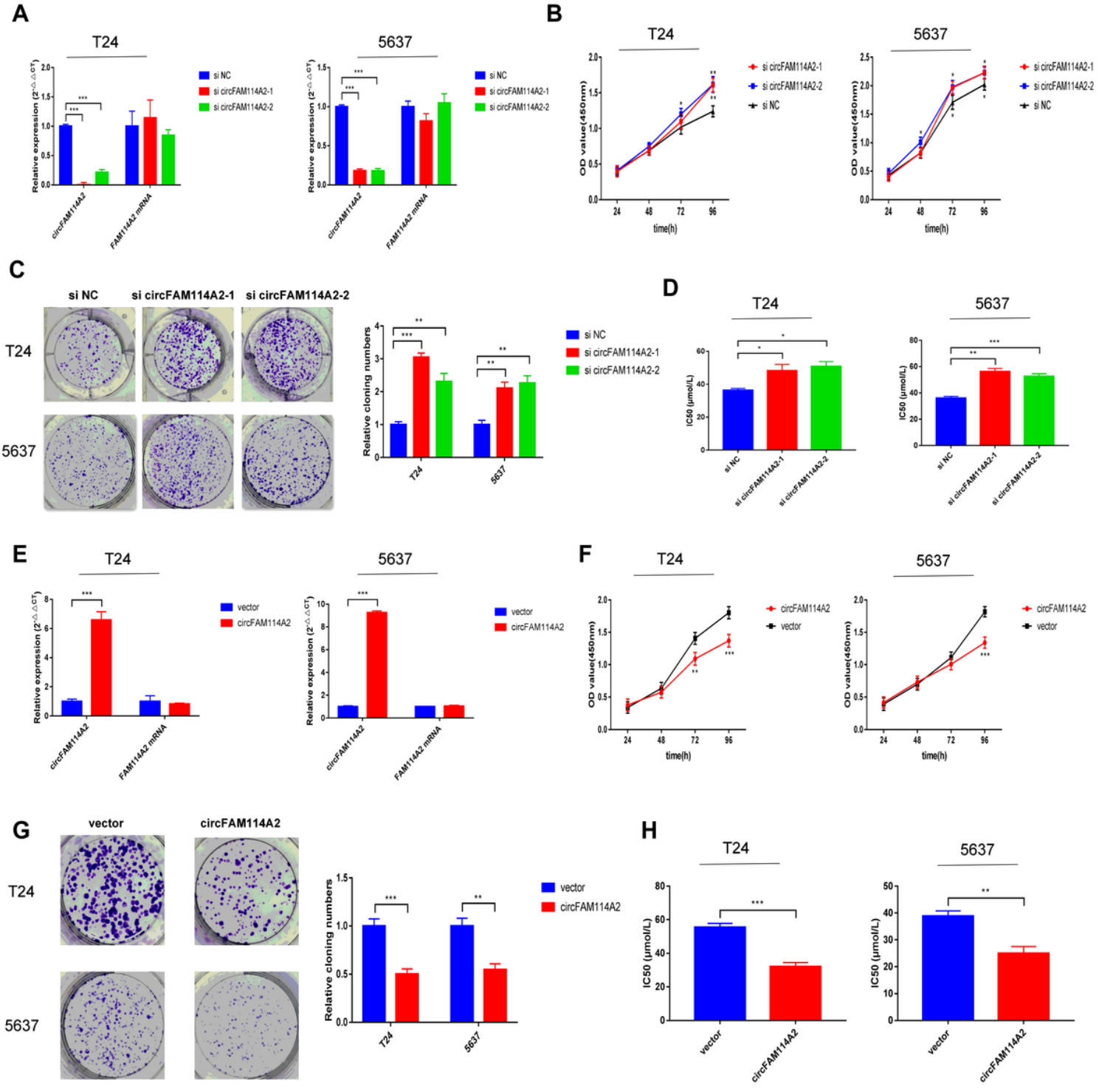

Figure 2

CircFAM114A2 could inhibit BCa proliferation and increase the sensitivity of BCa cells to cisplatin in vitro. A Two siRNAs vectors specifically targeting circFAM114A2 and control vector (NC) were transfected into T24 and 5637 cells respectively. The interfering efficacy of each siRNA vector on circFAM114A2 and FAM114A2 mRNA was tested by qRT-PCR (***P<0.001, Student's t-test). B Knockdown of circFAM114A2 promoted cell proliferation as indicated by CCK-8 assays in T24 and 5637 cells (*P<0.05, **P<0.01, Student's t-test). C Colony formation assay showed that circFAM114A2 knockdown significantly increased the cloning number of T24 and 5637 cells compared with control group (**P<0.01, ***P<0.001, Student's t-test). D IC50 value showed that circFAM114A2 knockdown could reduce the sensitivity of T24 and 5637 cells to cisplatin (*P<0.05,**P<0.01,***P<0.001,Student's t-test). E The expression levels of circFAM114A2 and FAM114A2 mRNA in T24 and 5637 cells transfected with circFAM114A2 or control vector plasmids were detected by qRT-PCR (***P<0.001, Student's t-test). F Overexpression of circFAM114A2 inhibited cell proliferation as indicated by CCK-8 assays in T24 and 5637 cells (**P<0.01, ***P<0.001, Student's t-test). G Colony formation assay showed that overexpression of circFAM114A2 significantly decreased the cloning number of T24 and 5637 cells compared with control group (**P<0.01, ***P<0.001, Student's t-test). H IC50 value showed that overexpression of circFAM114A2 could increase the sensitivity of T24 and 5637 cells to cisplatin (**P<0.01, ***P<0.001, Student's t-test). Data are mean±SD, n=3

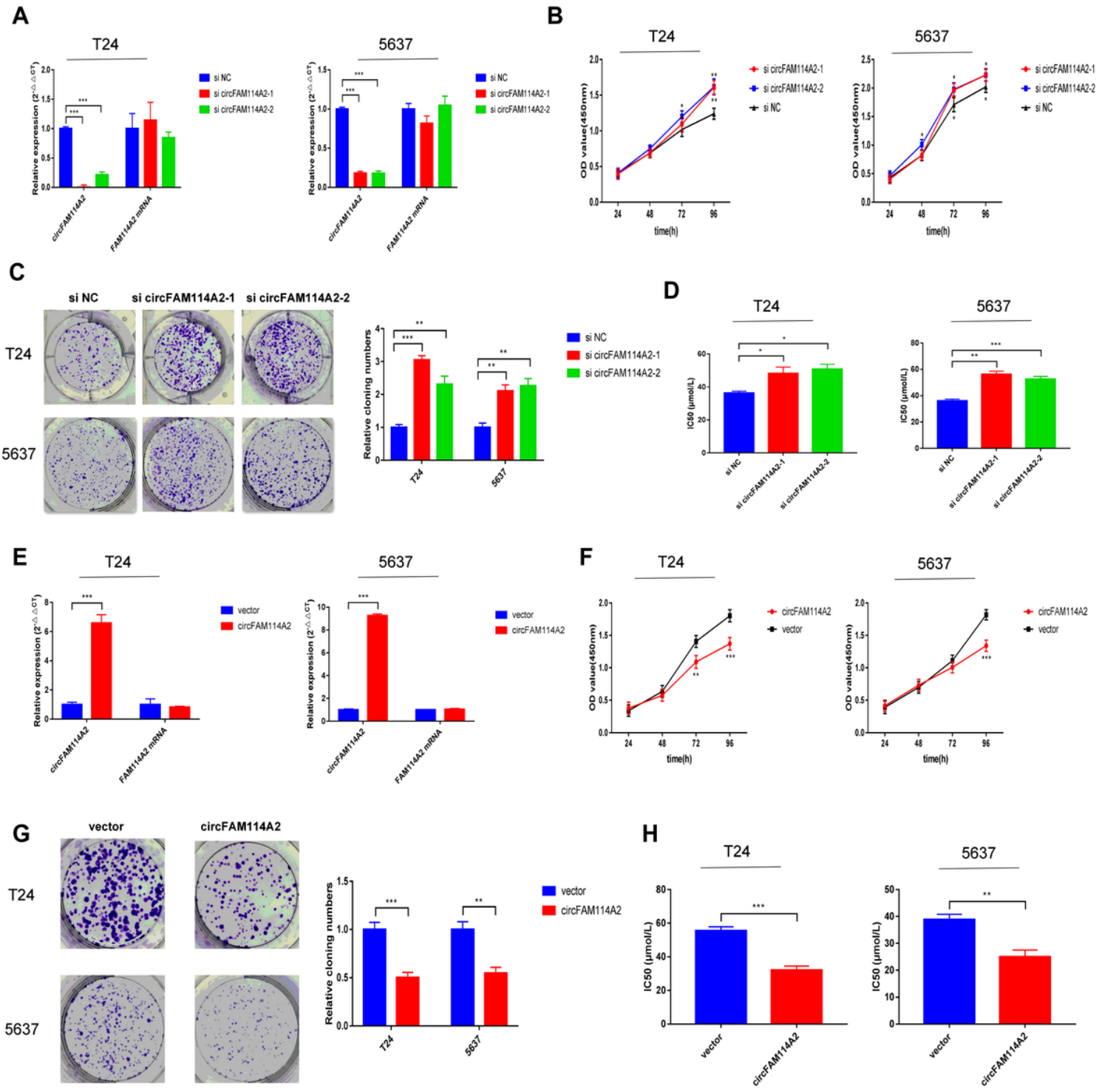

Figure 2

CircFAM114A2 could inhibit BCa proliferation and increase the sensitivity of BCa cells to cisplatin in vitro. A Two siRNAs vectors specifically targeting circFAM114A2 and control vector (NC) were transfected into T24 and 5637 cells respectively. The interfering efficacy of each siRNA vector on circFAM114A2 and FAM114A2 mRNA was tested by qRT-PCR (***P<0.001, Student's t-test). B Knockdown of circFAM114A2 promoted cell proliferation as indicated by CCK-8 assays in T24 and 5637 cells (*P<0.05, **P<0.01, Student's t-test). C Colony formation assay showed that circFAM114A2 knockdown significantly

increased the cloning number of T24 and 5637 cells compared with control group (**P<0.01, ***P<0.001, Student's t-test). D IC50 value showed that circFAM114A2 knockdown could reduce the sensitivity of T24 and 5637 cells to cisplatin (*P<0.05,**P<0.01,***P<0.001,Student's t-test). E The expression levels of circFAM114A2 and FAM114A2 mRNA in T24 and 5637 cells transfected with circFAM114A2 or control vector plasmids were detected by qRT-PCR (***P<0.001, Student's t-test). F Overexpression of circFAM114A2 inhibited cell proliferation as indicated by CCK-8 assays in T24 and 5637 cells (**P<0.01, ***P<0.001, Student's t-test). G Colony formation assay showed that overexpression of circFAM114A2 significantly decreased the cloning number of T24 and 5637 cells compared with control group (**P<0.01, ***P<0.001, Student's t-test). H IC50 value showed that overexpression of circFAM114A2 could increase the sensitivity of T24 and 5637 cells to cisplatin (**P<0.01, ***P<0.001, Student's t-test). Data are mean±SD, n=3

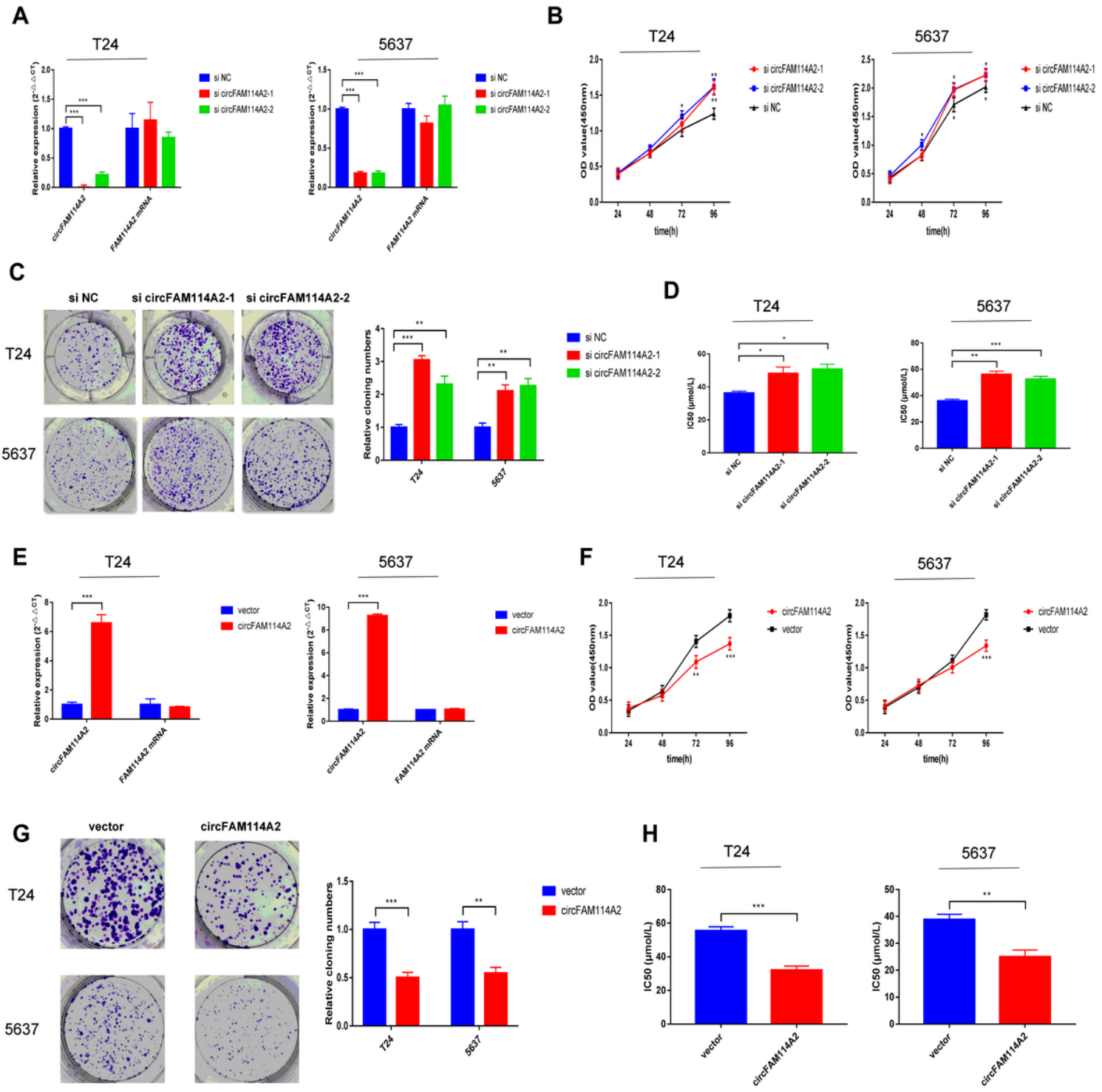

Figure 2

CircFAM114A2 could inhibit BCa proliferation and increase the sensitivity of BCa cells to cisplatin in vitro. A Two siRNAs vectors specifically targeting circFAM114A2 and control vector (NC) were transfected into T24 and 5637 cells respectively. The interfering efficacy of each siRNA vector on circFAM114A2 and FAM114A2 mRNA was tested by qRT-PCR (***P<0.001, Student's t-test). B Knockdown of circFAM114A2 promoted cell proliferation as indicated by CCK-8 assays in T24 and 5637 cells (*P<0.05, **P<0.01, Student's t-test). C Colony formation assay showed that circFAM114A2 knockdown significantly

increased the cloning number of T24 and 5637 cells compared with control group (**P<0.01, ***P<0.001, Student’s t-test). D IC50 value showed that circFAM114A2 knockdown could reduce the sensitivity of T24 and 5637 cells to cisplatin (*P<0.05,**P<0.01,***P<0.001,Student’s t-test). E The expression levels of circFAM114A2 and FAM114A2 mRNA in T24 and 5637 cells transfected with circFAM114A2 or control vector plasmids were detected by qRT-PCR (***P<0.001, Student’s t-test). F Overexpression of circFAM114A2 inhibited cell proliferation as indicated by CCK-8 assays in T24 and 5637 cells (**P<0.01, ***P<0.001, Student’s t-test). G Colony formation assay showed that overexpression of circFAM114A2 significantly decreased the cloning number of T24 and 5637 cells compared with control group (**P<0.01, ***P<0.001, Student’s t-test). H IC50 value showed that overexpression of circFAM114A2 could increase the sensitivity of T24 and 5637 cells to cisplatin (**P<0.01, ***P<0.001, Student’s t-test). Data are mean±SD, n=3

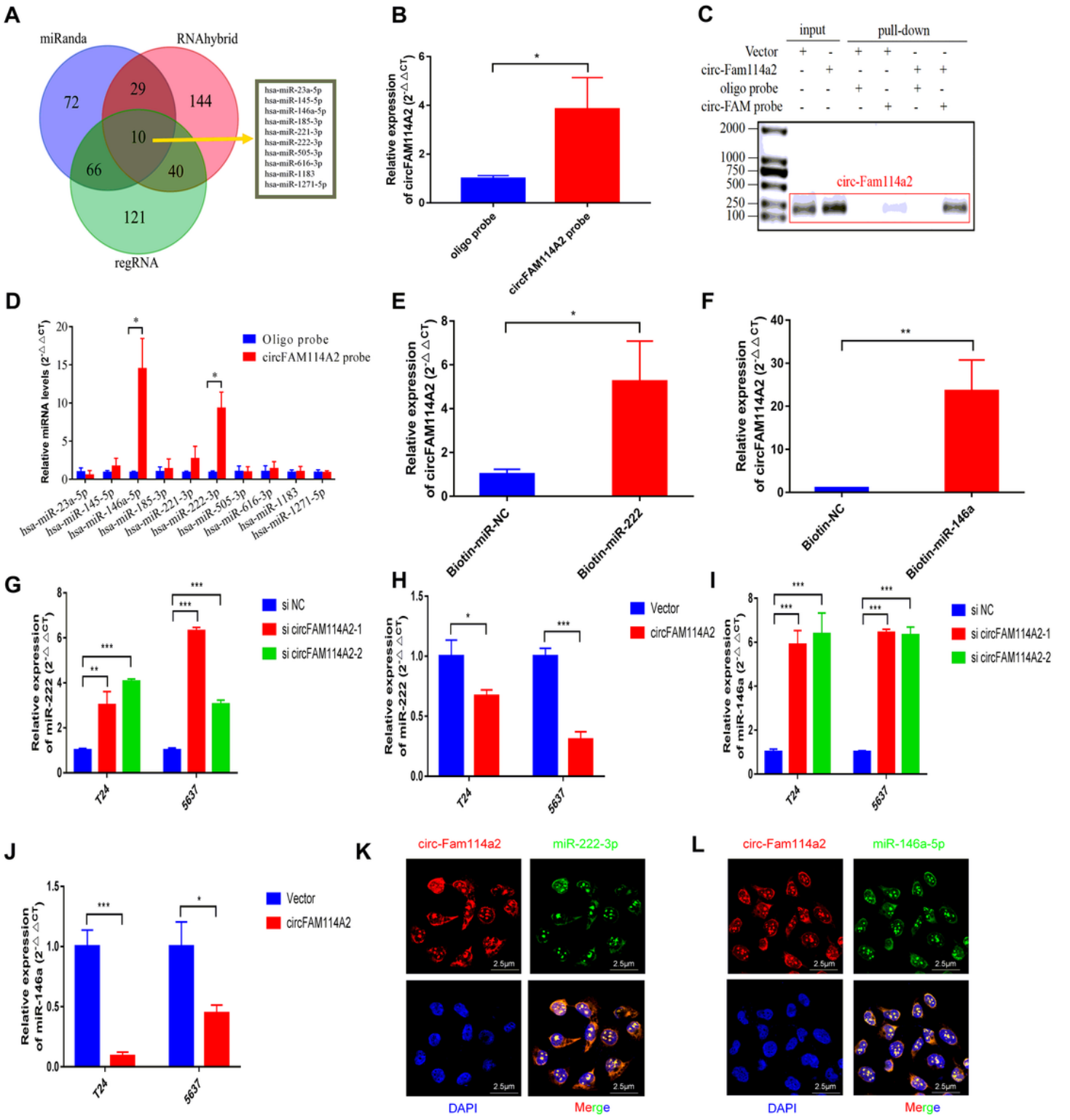

Figure 3

CircFAM114A2 acts as a sponge for miR-222-3p and miR-146a-5p in BCa cells. A Schematic illustration showed overlapping of the target miRNAs of circFAM114A2 predicted by miRanda, regRNA and RNAhybrid. B and C CircFAM114A2 in BCa cell lysates was pulled down and enriched with circFAM114A2 specific probe and then detected by qRT-PCR. Relative level of circFAM114A2 was normalized to input. GAPDH was used as negative control (*P<0.05, Student's t-test). D The relative levels of 10 miRNA

candidates in the BCa cell lysates were detected by qRT-PCR. And miR-222-3p and miR-146a-5p were pulled down by circFAM114A2 probe (*P<0.05, Student's t-test). E and F Biotin-coupled miR-222-3p/miR-146a-5p captured a fold change of circFAM114A2 in the complex as compared with biotin-coupled NC in biotin-coupled miRNA capture (*P<0.05, **P<0.01, Student's t-test). G and H The expression level of miR-222-3p was influenced by circFAM114A2 detected by qRT-PCR (*P<0.05, **P<0.01, ***P<0.001, Student's t-test). I and J The expression level of miR-146a-5p was influenced by circFAM114A2 detected by qRT-PCR (*P<0.05, **P<0.01, ***P<0.001, Student's t-test). Data are mean±SD, n=3. K and L RNA FISH for circFAM114A2 and miR-222-3p/miR-146a-5p was detected in T24. Nuclei was stained blue (DAPI), circFAM114A2 was stained red, and miR-222-3p/miR-146a-5p were stained green.

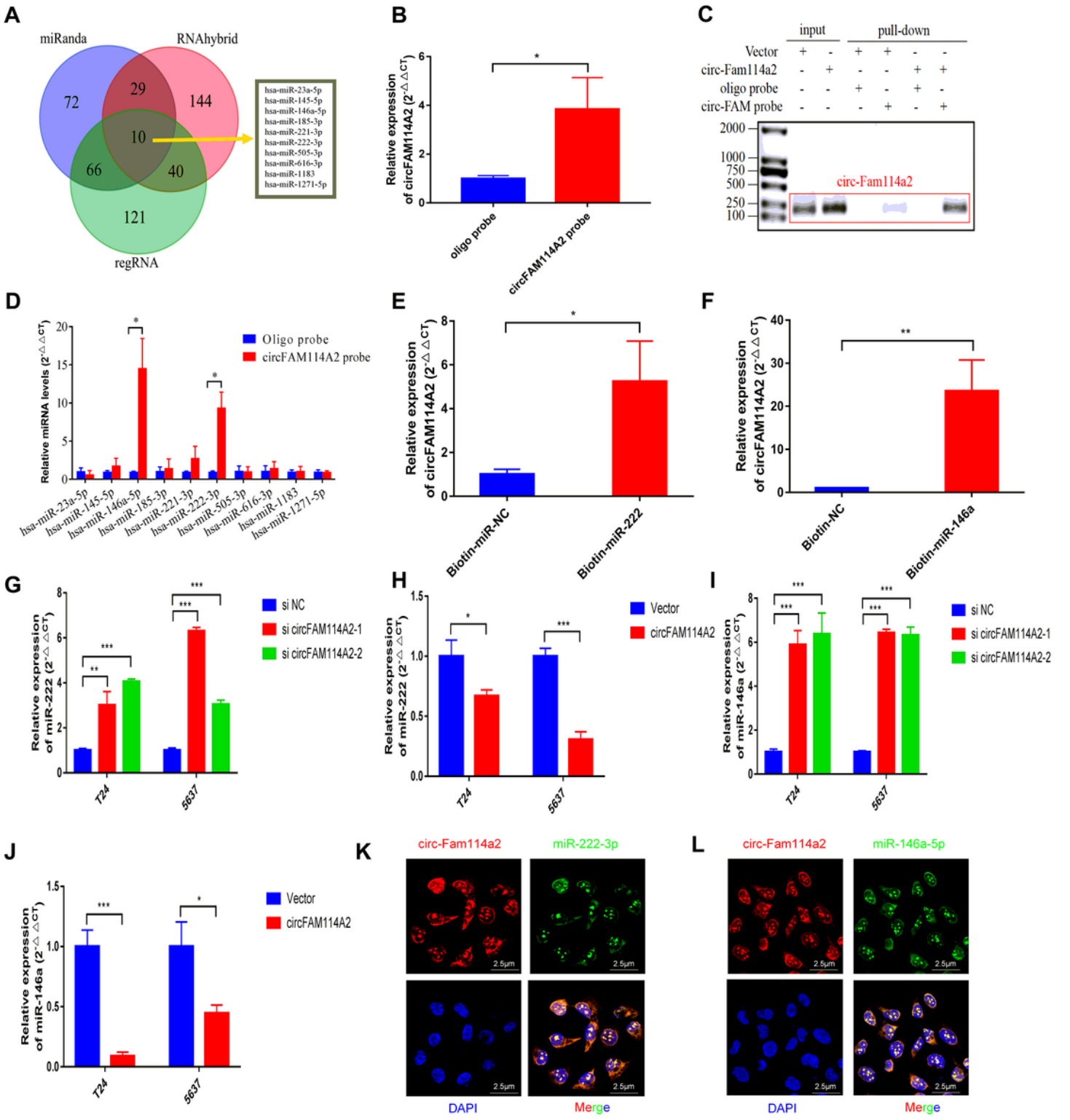

Figure 3

CircFAM114A2 acts as a sponge for miR-222-3p and miR-146a-5p in BCa cells. A Schematic illustration showed overlapping of the target miRNAs of circFAM114A2 predicted by miRanda, regRNA and RNAhybrid. B and C CircFAM114A2 in BCa cell lysates was pulled down and enriched with circFAM114A2 specific probe and then detected by qRT-PCR. Relative level of circFAM114A2 was normalized to input. GAPDH was used as negative control (*P<0.05, Student's t-test). D The relative levels of 10 miRNA

candidates in the BCa cell lysates were detected by qRT-PCR. And miR-222-3p and miR-146a-5p were pulled down by circFAM114A2 probe (*P<0.05, Student's t-test). E and F Biotin-coupled miR-222-3p/miR-146a-5p captured a fold change of circFAM114A2 in the complex as compared with biotin-coupled NC in biotin-coupled miRNA capture (*P<0.05, **P<0.01, Student's t-test). G and H The expression level of miR-222-3p was influenced by circFAM114A2 detected by qRT-PCR (*P<0.05, **P<0.01, ***P<0.001, Student's t-test). I and J The expression level of miR-146a-5p was influenced by circFAM114A2 detected by qRT-PCR (*P<0.05, **P<0.01, ***P<0.001, Student's t-test). Data are mean±SD, n=3. K and L RNA FISH for circFAM114A2 and miR-222-3p/miR-146a-5p was detected in T24. Nuclei was stained blue (DAPI), circFAM114A2 was stained red, and miR-222-3p/miR-146a-5p were stained green.

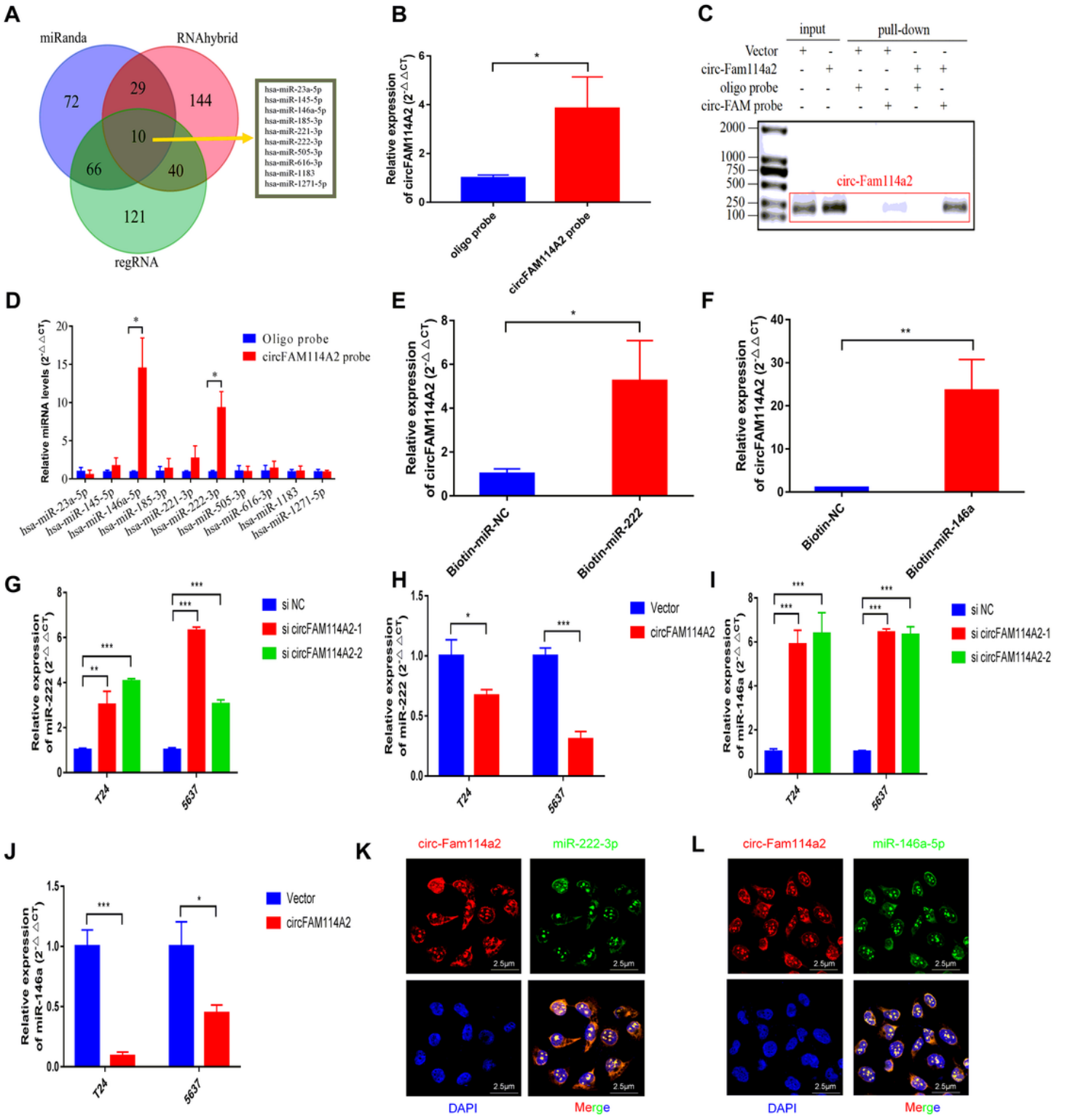

Figure 3

CircFAM114A2 acts as a sponge for miR-222-3p and miR-146a-5p in BCa cells. A Schematic illustration showed overlapping of the target miRNAs of circFAM114A2 predicted by miRanda, regRNA and RNAhybrid. B and C CircFAM114A2 in BCa cell lysates was pulled down and enriched with circFAM114A2 specific probe and then detected by qRT-PCR. Relative level of circFAM114A2 was normalized to input. GAPDH was used as negative control (*P<0.05, Student's t-test). D The relative levels of 10 miRNA

candidates in the BCa cell lysates were detected by qRT-PCR. And miR-222-3p and miR-146a-5p were pulled down by circFAM114A2 probe (*P<0.05, Student's t-test). E and F Biotin-coupled miR-222-3p/miR-146a-5p captured a fold change of circFAM114A2 in the complex as compared with biotin-coupled NC in biotin-coupled miRNA capture (*P<0.05, **P<0.01, Student's t-test). G and H The expression level of miR-222-3p was influenced by circFAM114A2 detected by qRT-PCR (*P<0.05, **P<0.01, ***P<0.001, Student's t-test). I and J The expression level of miR-146a-5p was influenced by circFAM114A2 detected by qRT-PCR (*P<0.05, **P<0.01, ***P<0.001, Student's t-test). Data are mean±SD, n=3. K and L RNA FISH for circFAM114A2 and miR-222-3p/miR-146a-5p was detected in T24. Nuclei was stained blue (DAPI), circFAM114A2 was stained red, and miR-222-3p/miR-146a-5p were stained green.

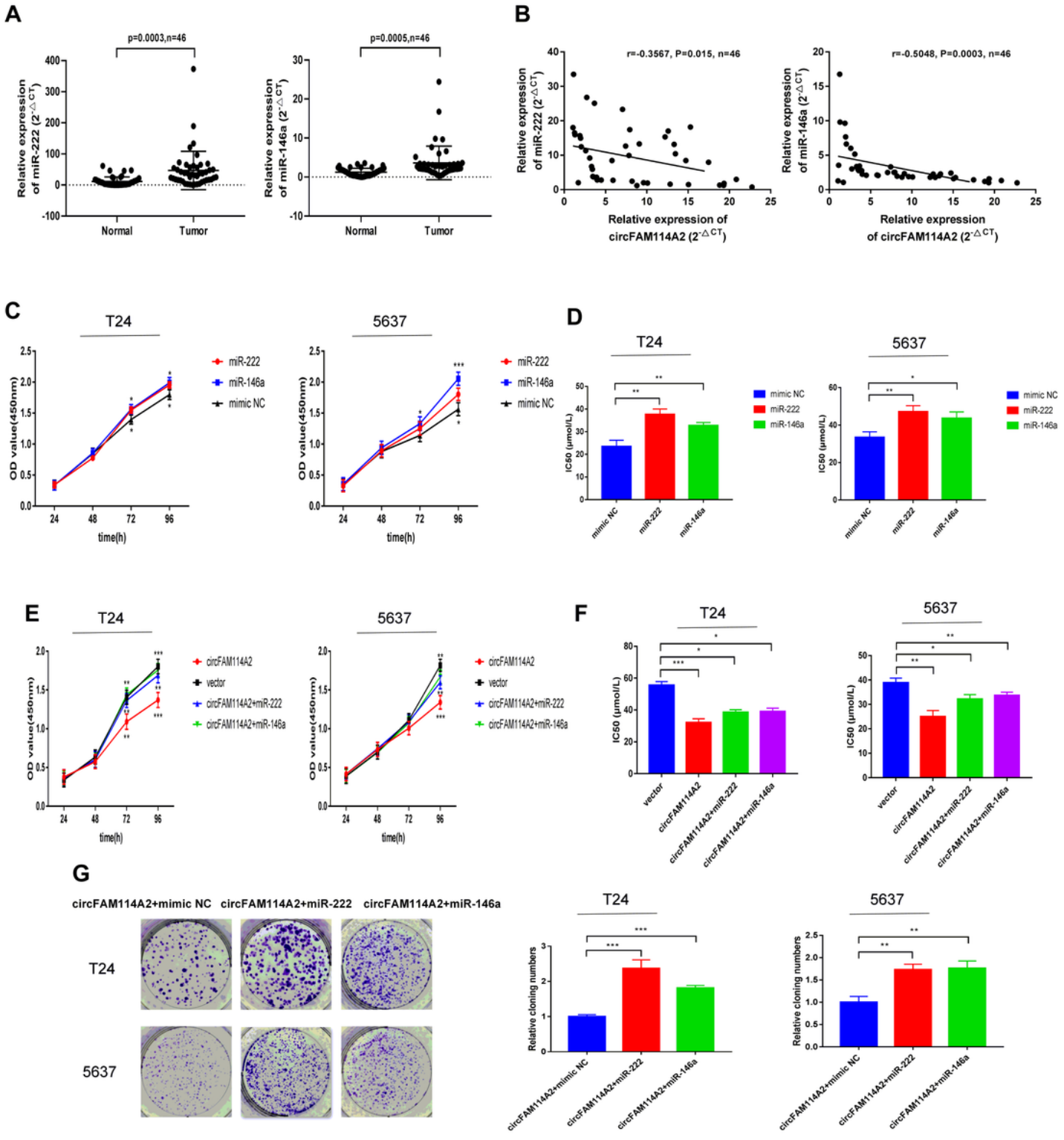

Figure 4

MIR-222-3p/miR-146a-5p played as oncogenes and transfection of miR-222-3p/miR-146a-5p mimic eliminated the repression function of circFAM114A2. A QRT-PCR revealed that miR-222-3p and miR-146a-5p were up-regulated in BCa tissues (n=46) compared with normal adjacent bladder tissues. B A negative correlation between the expression of circFAM114A2 and miR-222-3p/miR-146a-5p was showed using Pearson correlation analysis. C CCK-8 assay showed that miR-222-3p and miR-146a-5p promoted the

proliferation of T24 and 5637 cells (*P<0.05, ***P<0.001, Student's t-test). D IC50 value showed that overexpression of miR-222-3p and miR-146a-5p could decrease the sensitivity of T24 and 5637 cells to cisplatin (*P<0.05, **P<0.01, Student's t-test). E CCK-8 assays showed that co-transfected with miR-222-3p or miR-146a-5p mimic could reverse proliferation-repression function of circFAM114A2 in T24 and 5637 cells (**P<0.01, ***P<0.001, Student's t-test). F IC50 value showed that co-transfected with miR-222-3p or miR-146a-5p mimic could reverse the increasing sensitivity to cisplatin induced by circFAM114A2 in T24 and 5637 cells (*P<0.05, **P<0.01, ***P<0.001, Student's t-test). G Colony formation assay showed that co-transfecting with miR-222-3p or miR-146a-5p mimic could reverse the decreasing cloning number of T24 and 5637 cells caused by circFAM114A2 (**P<0.01, ***P<0.001, Student's t-test). Data are mean±SD, n=3

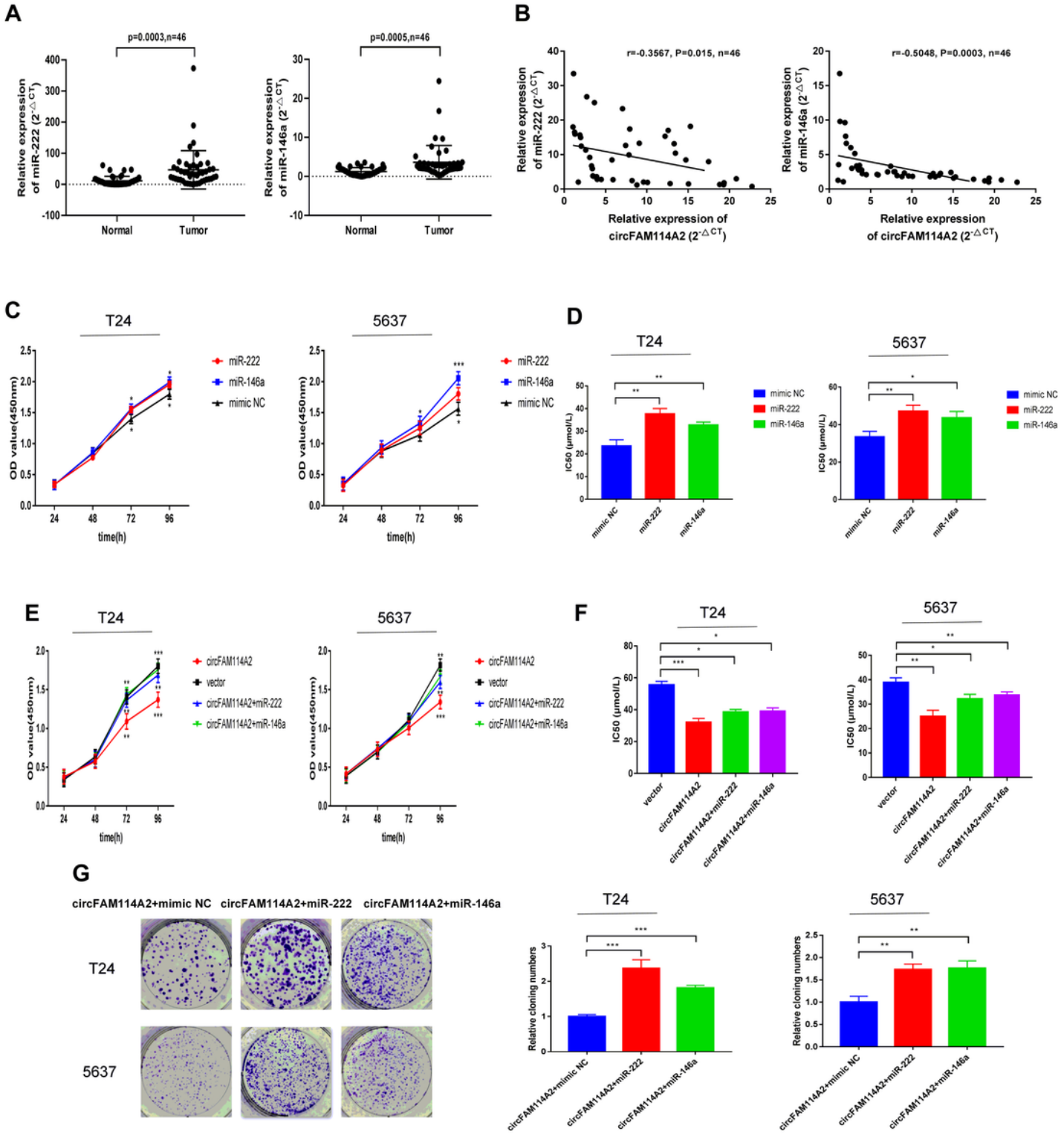

Figure 4

MIR-222-3p/miR-146a-5p played as oncogenes and transfection of miR-222-3p/miR-146a-5p mimic eliminated the repression function of circFAM114A2. A QRT-PCR revealed that miR-222-3p and miR-146a-5p were up-regulated in BCa tissues (n=46) compared with normal adjacent bladder tissues. B A negative correlation between the expression of circFAM114A2 and miR-222-3p/miR-146a-5p was showed using Pearson correlation analysis. C CCK-8 assay showed that miR-222-3p and miR-146a-5p promoted the

proliferation of T24 and 5637 cells (*P<0.05, ***P<0.001, Student's t-test). D IC50 value showed that overexpression of miR-222-3p and miR-146a-5p could decrease the sensitivity of T24 and 5637 cells to cisplatin (*P<0.05, **P<0.01, Student's t-test). E CCK-8 assays showed that co-transfected with miR-222-3p or miR-146a-5p mimic could reverse proliferation-repression function of circFAM114A2 in T24 and 5637 cells (**P<0.01, ***P<0.001, Student's t-test). F IC50 value showed that co-transfected with miR-222-3p or miR-146a-5p mimic could reverse the increasing sensitivity to cisplatin induced by circFAM114A2 in T24 and 5637 cells (*P<0.05, **P<0.01, ***P<0.001, Student's t-test). G Colony formation assay showed that co-transfecting with miR-222-3p or miR-146a-5p mimic could reverse the decreasing cloning number of T24 and 5637 cells caused by circFAM114A2 (**P<0.01, ***P<0.001, Student's t-test). Data are mean±SD, n=3

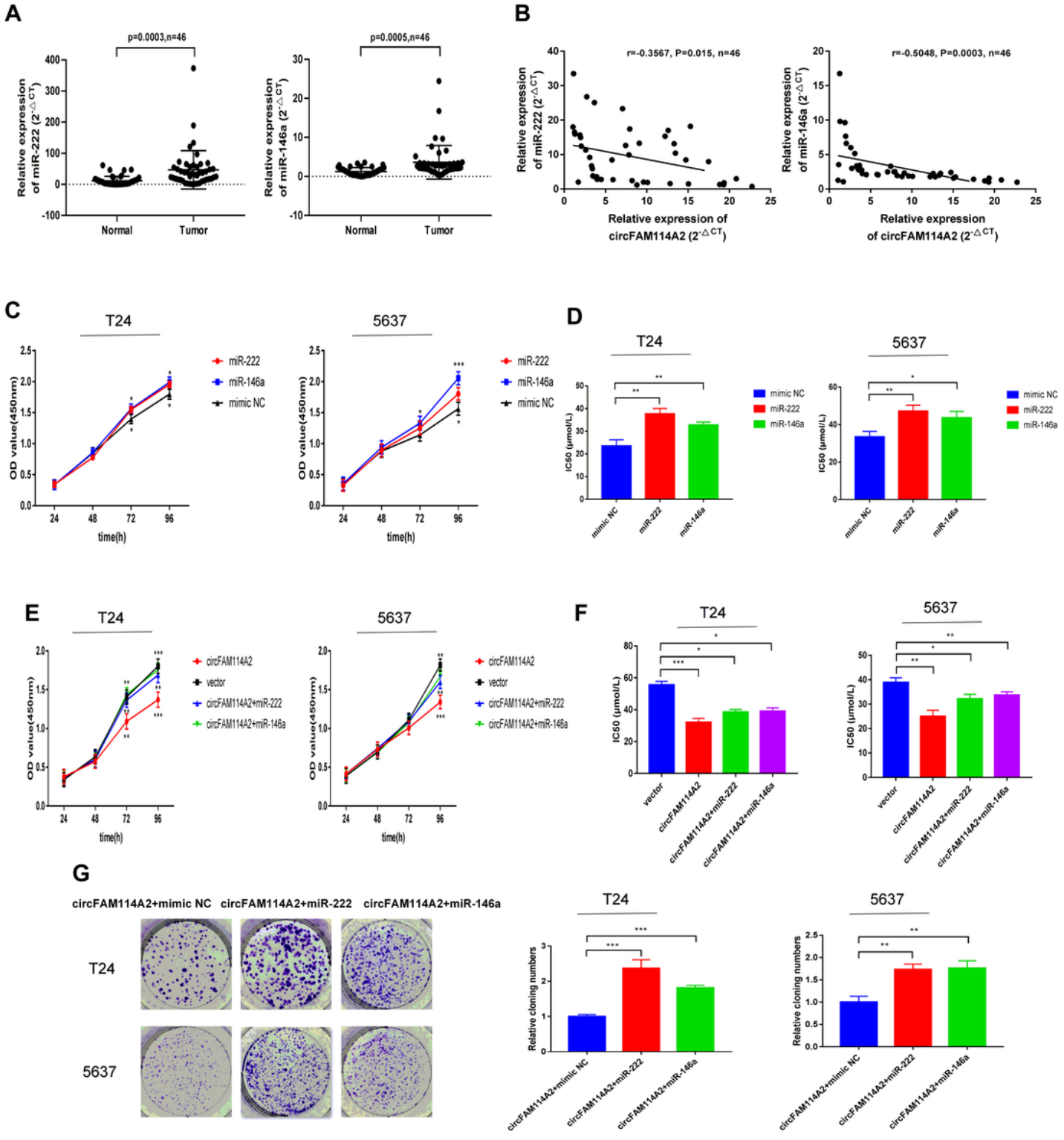

Figure 4

MIR-222-3p/miR-146a-5p played as oncogenes and transfection of miR-222-3p/miR-146a-5p mimic eliminated the repression function of circFAM114A2. A QRT-PCR revealed that miR-222-3p and miR-146a-5p were up-regulated in BCa tissues (n=46) compared with normal adjacent bladder tissues. B A negative correlation between the expression of circFAM114A2 and miR-222-3p/miR-146a-5p was showed using Pearson correlation analysis. C CCK-8 assay showed that miR-222-3p and miR-146a-5p promoted the

proliferation of T24 and 5637 cells (*P<0.05, ***P<0.001, Student's t-test). D IC50 value showed that overexpression of miR-222-3p and miR-146a-5p could decrease the sensitivity of T24 and 5637 cells to cisplatin (*P<0.05, **P<0.01, Student's t-test). E CCK-8 assays showed that co-transfected with miR-222-3p or miR-146a-5p mimic could reverse proliferation-repression function of circFAM114A2 in T24 and 5637 cells (**P<0.01, ***P<0.001, Student's t-test). F IC50 value showed that co-transfected with miR-222-3p or miR-146a-5p mimic could reverse the increasing sensitivity to cisplatin induced by circFAM114A2 in T24 and 5637 cells (*P<0.05, **P<0.01, ***P<0.001, Student's t-test). G Colony formation assay showed that co-transfecting with miR-222-3p or miR-146a-5p mimic could reverse the decreasing cloning number of T24 and 5637 cells caused by circFAM114A2 (**P<0.01, ***P<0.001, Student's t-test). Data are mean±SD, n=3

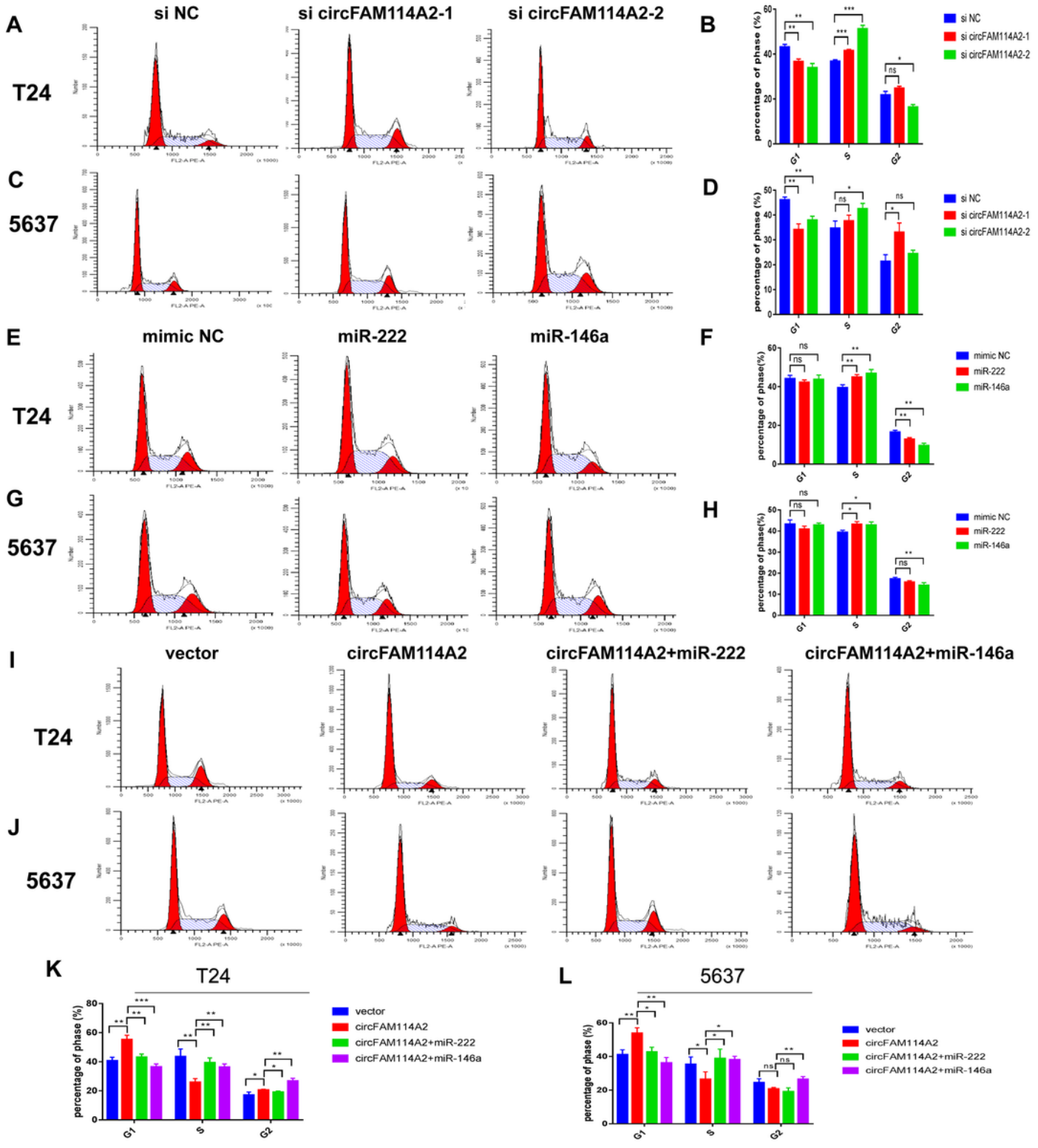

Figure 5

MiR-222-3p/miR-146a-5p could rescue cell cycle arrest induce by circFAM114A2 A–D Less cells were distributed in G1 phase and more cells were distributed in S phase of circFAM114A2 knockdown group comparing with control group in T24 and 5637 cell lines (*P<0.05, **P<0.01, ***P<0.001, Student's t-test). E-H More cells were distributed in S phase of miR-222-3p/miR-146a-5p mimic group compared with control group in T24 and 5637 cell lines (*P<0.05, **P<0.01, ***P<0.001, Student's t-test). I-L More cells

were distributed in G1 phase and less cells were distributed in S phase in circFAM114A2 overexpression group comparing with control group in T24 and 5637 cells, and miR-222-3p and miR-146a-5p mimic transfection could reverse the G1 phase redundant and reduced S phase (*P<0.05, **P<0.01, ***P<0.001, Student's t-test). Data are mean±SD, n=3

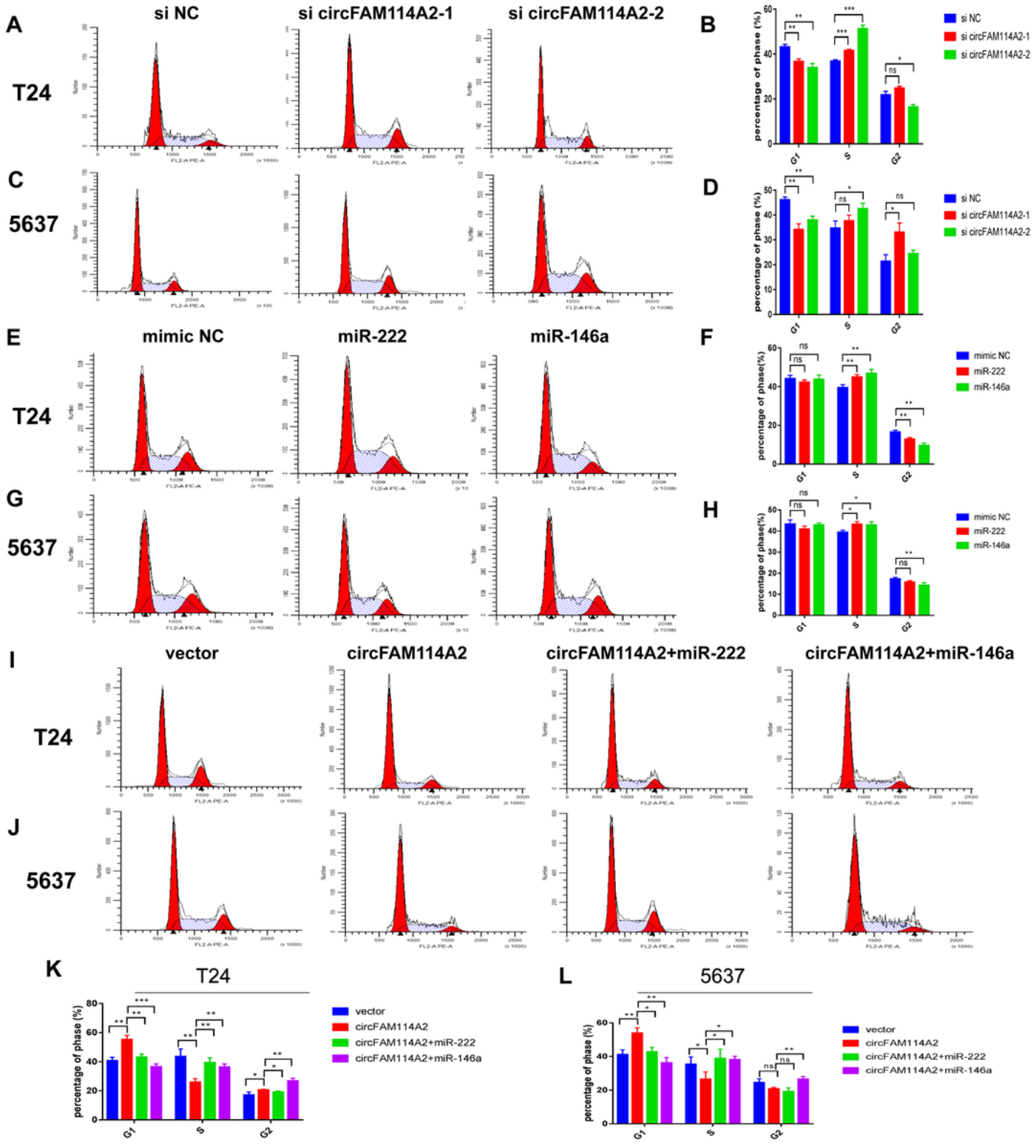

Figure 5

MiR-222-3p/miR-146a-5p could rescue cell cycle arrest induce by circFAM114A2 A–D Less cells were distributed in G1 phase and more cells were distributed in S phase of circFAM114A2 knockdown group comparing with control group in T24 and 5637 cell lines (*P<0.05, **P<0.01, ***P<0.001, Student's t-test). E-H More cells were distributed in S phase of miR-222-3p/miR-146a-5p mimic group compared with control group in T24 and 5637 cell lines (*P<0.05, **P<0.01, ***P<0.001, Student's t-test). I-L More cells were distributed in G1 phase and less cells were distributed in S phase in circFAM114A2 overexpression group comparing with control group in T24 and 5637 cells, and miR-222-3p and miR-146a-5p mimic transfection could reverse the G1 phase redundant and reduced S phase (*P<0.05, **P<0.01, ***P<0.001, Student's t-test). Data are mean±SD, n=3

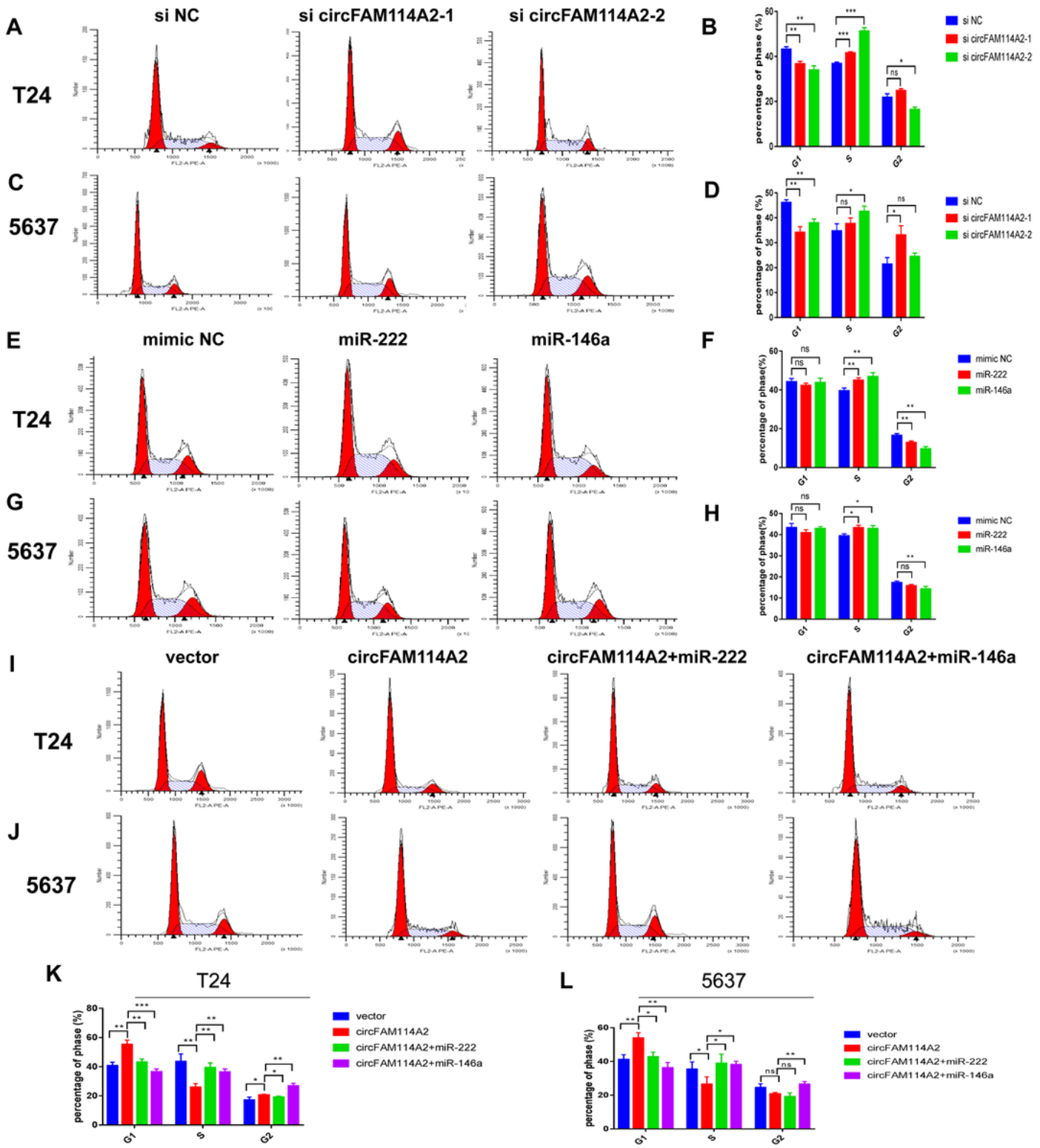

Figure 5

MiR-222-3p/miR-146a-5p could rescue cell cycle arrest induce by circFAM114A2 A–D Less cells were distributed in G1 phase and more cells were distributed in S phase of circFAM114A2 knockdown group comparing with control group in T24 and 5637 cell lines (*P<0.05, **P<0.01, ***P<0.001, Student's t-test). E-H More cells were distributed in S phase of miR-222-3p/miR-146a-5p mimic group compared with control group in T24 and 5637 cell lines (*P<0.05, **P<0.01, ***P<0.001, Student's t-test). I-L More cells

were distributed in G1 phase and less cells were distributed in S phase in circFAM114A2 overexpression group comparing with control group in T24 and 5637 cells, and miR-222-3p and miR-146a-5p mimic transfection could reverse the G1 phase redundant and reduced S phase (*P<0.05, **P<0.01, ***P<0.001, Student's t-test). Data are mean±SD, n=3

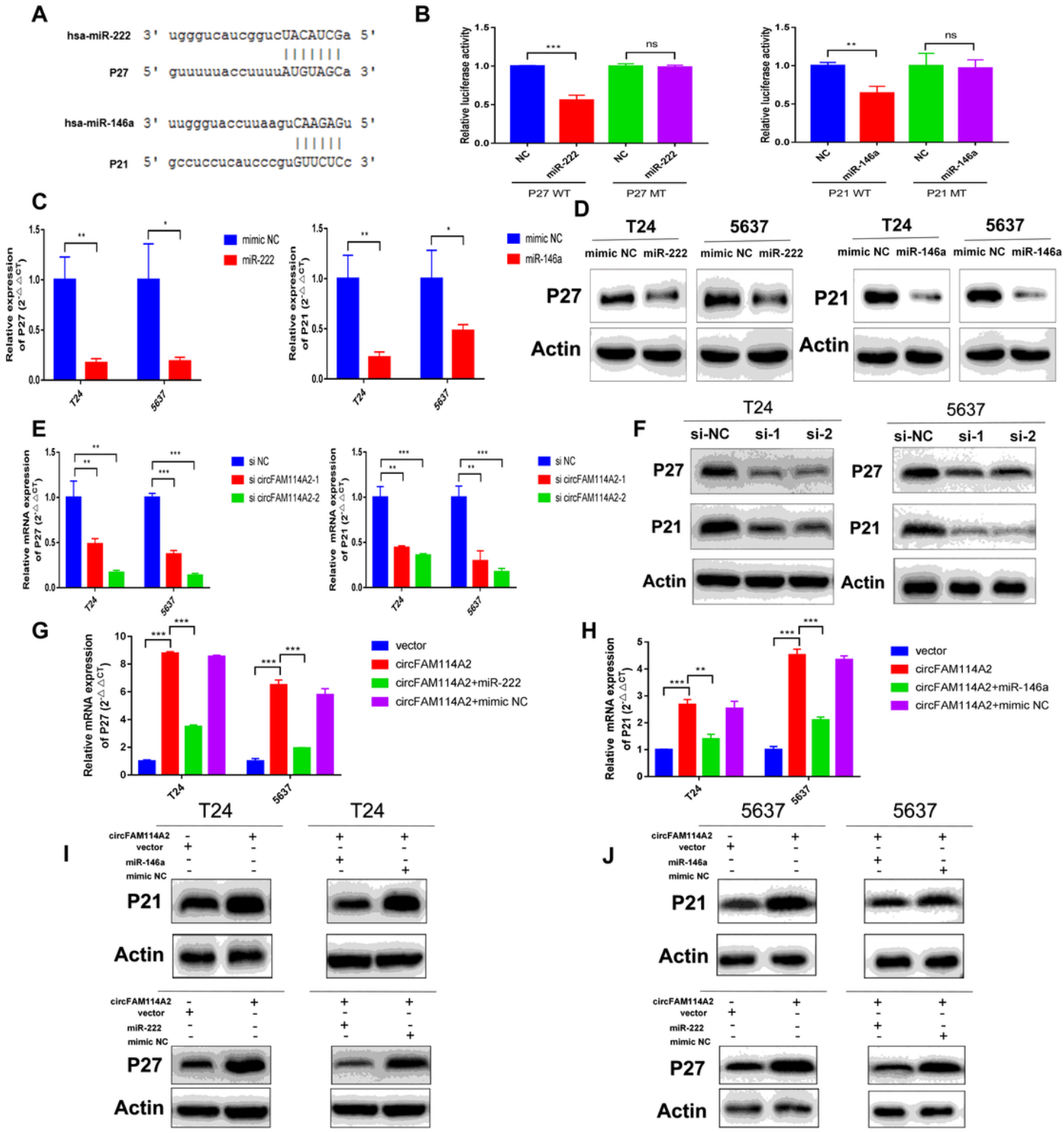

Figure 6

MIR-222-3p/miR-146a-5p promoted BCa progression through targeting P27 and P21 respectively. A Predicted miR-222-3p/miR-146a-5p binding sites in the 3'-UTR of P27/P21 mRNA by bioinformatics analysis. B Dual luciferase reporter assays demonstrated that P27 and P21 are direct target of miR-222-3p and miR-146a-5p (**P<0.01,***P<0.001,Student’s t-test). C miR-222-3p/miR-146a-5p could reduce the expression of P27/P21 in T24 and 5637 cells detected by qRT-PCR (*P<0.05, **P<0.01, Student’s t-test). D miR-222-3p/miR-146a-5p could reduce the expression of P27/P21 in T24 and 5637 cells detected by western blot. E Knockdown of circFAM114A2 down-regulated the mRNA expression level of P27 and P21 in T24 and 5637 cells by qRT-PCR (**P<0.01, ***P<0.001, Student’s t-test). F Knockdown of circFAM114A2 down-regulated the protein expression level of P27 and P21 by western blot. G and H Overexpression of circFAM114A2 up-regulated the mRNA expression level of P27 and P21 in T24 and 5637 cells by qRT-PCR, and co-transfection of miR222 and miR146a could reverse it respectively. (**P<0.01, ***P<0.001, Student’s t-test). I and J Overexpression of circFAM114A2 up-regulated the protein expression level of P27 and P21 by western blot, and co-transfection of miR222 and miR146a could reverse it respectively. Data are mean±SD, n=3

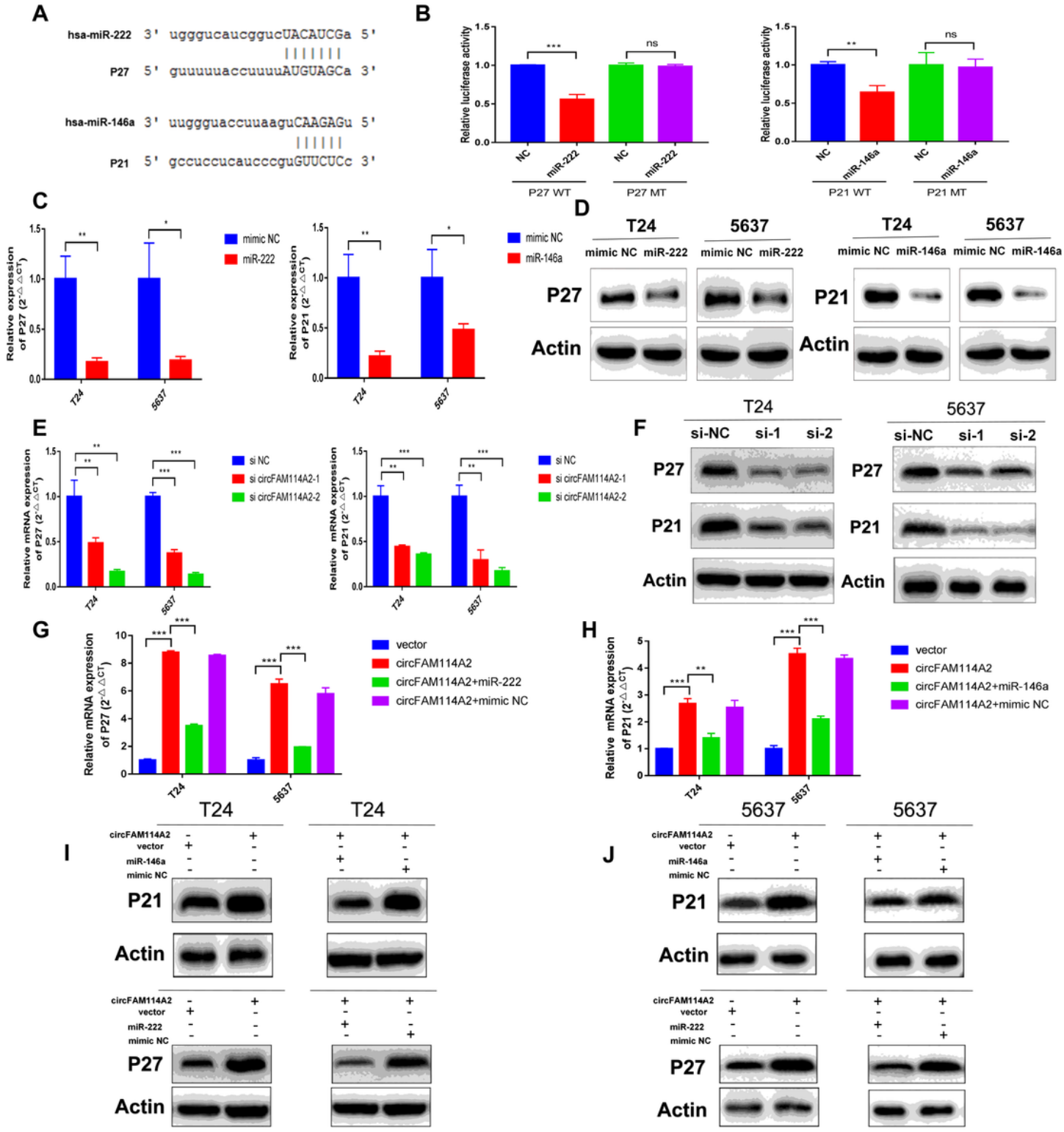

Figure 6

MIR-222-3p/miR-146a-5p promoted BCa progression through targeting P27 and P21 respectively. A Predicted miR-222-3p/miR-146a-5p binding sites in the 3'-UTR of P27/P21 mRNA by bioinformatics analysis. B Dual luciferase reporter assays demonstrated that P27 and P21 are direct target of miR-222-3p and miR-146a-5p (**P<0.01,***P<0.001,Student's t-test). C miR-222-3p/miR-146a-5p could reduce the expression of P27/P21 in T24 and 5637 cells detected by qRT-PCR (*P<0.05, **P<0.01, Student's t-test). D

miR-222-3p/miR-146a-5p could reduce the expression of P27/P21 in T24 and 5637 cells detected by western blot. E Knockdown of circFAM114A2 down-regulated the mRNA expression level of P27 and P21 in T24 and 5637 cells by qRT-PCR (**P<0.01, ***P<0.001, Student's t-test). F Knockdown of circFAM114A2 down-regulated the protein expression level of P27 and P21 by western blot. G and H Overexpression of circFAM114A2 up-regulated the mRNA expression level of P27 and P21 in T24 and 5637 cells by qRT-PCR, and co-transfection of miR222 and miR146a could reverse it respectively. (**P<0.01, ***P<0.001, Student's t-test). I and J Overexpression of circFAM114A2 up-regulated the protein expression level of P27 and P21 by western blot, and co-transfection of miR222 and miR146a could reverse it respectively. Data are mean±SD, n=3

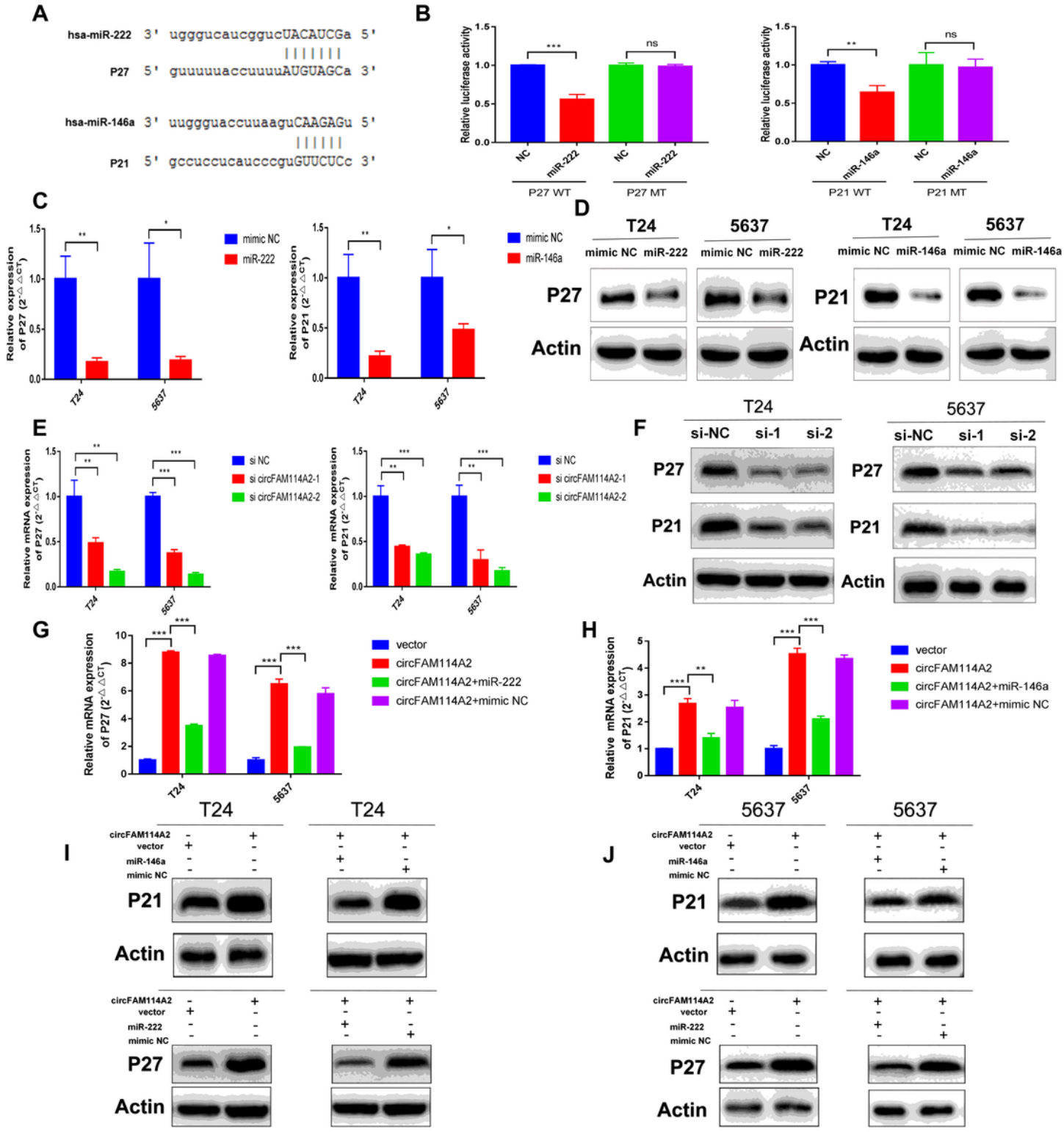

Figure 6

MIR-222-3p/miR-146a-5p promoted BCa progression through targeting P27 and P21 respectively. A Predicted miR-222-3p/miR-146a-5p binding sites in the 3'-UTR of P27/P21 mRNA by bioinformatics analysis. B Dual luciferase reporter assays demonstrated that P27 and P21 are direct target of miR-222-3p and miR-146a-5p (**P<0.01,***P<0.001,Student's t-test). C miR-222-3p/miR-146a-5p could reduce the expression of P27/P21 in T24 and 5637 cells detected by qRT-PCR (*P<0.05, **P<0.01, Student's t-test). D

miR-222-3p/miR-146a-5p could reduce the expression of P27/P21 in T24 and 5637 cells detected by western blot. E Knockdown of circFAM114A2 down-regulated the mRNA expression level of P27 and P21 in T24 and 5637 cells by qRT-PCR (**P<0.01, ***P<0.001, Student's t-test). F Knockdown of circFAM114A2 down-regulated the protein expression level of P27 and P21 by western blot. G and H Overexpression of circFAM114A2 up-regulated the mRNA expression level of P27 and P21 in T24 and 5637 cells by qRT-PCR, and co-transfection of miR222 and miR146a could reverse it respectively. (**P<0.01, ***P<0.001, Student's t-test). I and J Overexpression of circFAM114A2 up-regulated the protein expression level of P27 and P21 by western blot, and co-transfection of miR222 and miR146a could reverse it respectively. Data are mean±SD, n=3

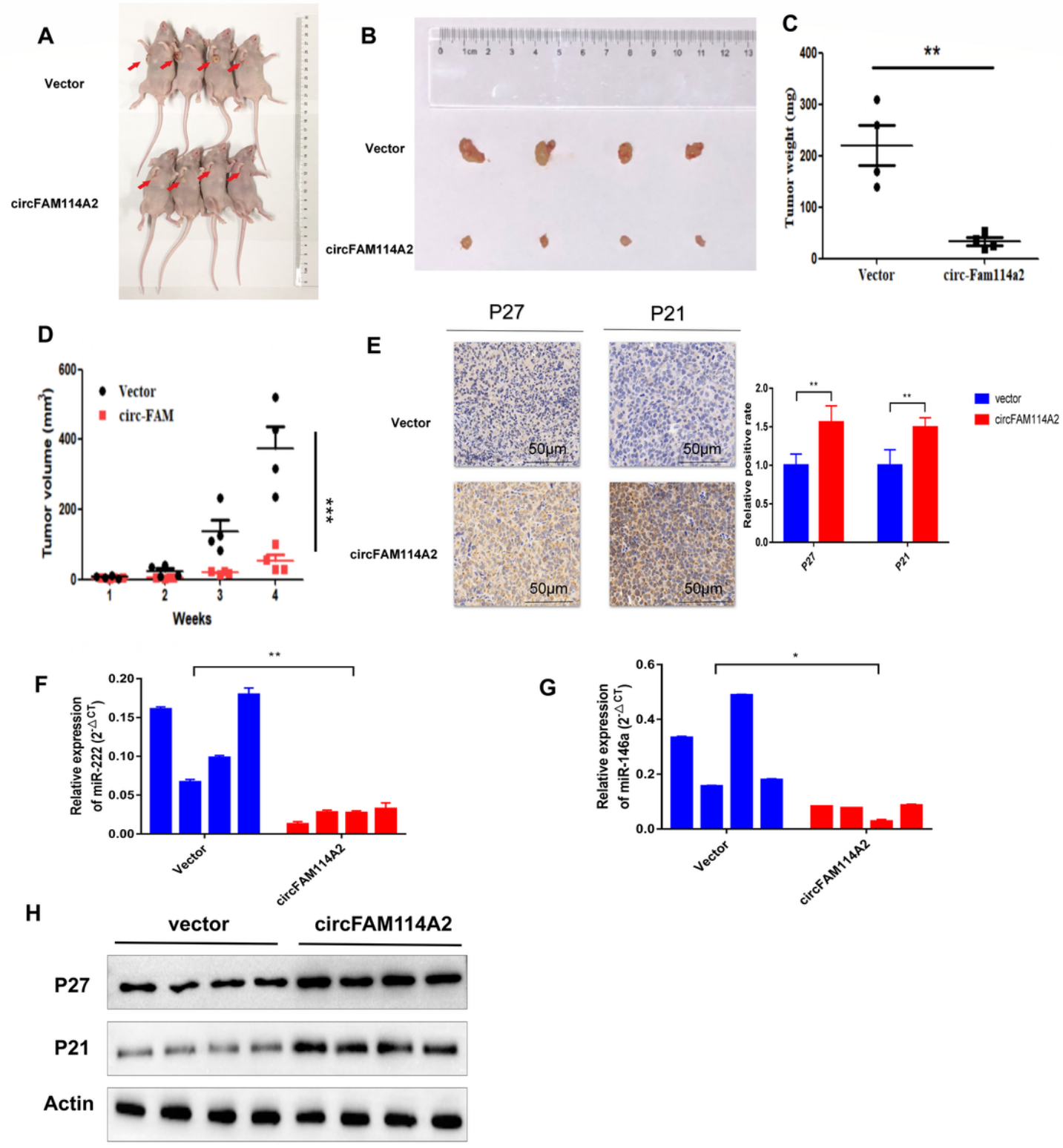

Figure 7

CircFAM114A2 suppressed tumor formation of xenograft in nude mice. A Representative image of the nude mice injected with circFAM114A2 or vector transfection T24 cells (n=4). B Representation picture of tumor formation of xenograft in nude mice injected with circFAM114A2 or vector transfection T24 cells (n=4). C Weights of tumors in two groups were measured using electronic scales (**P<0.01, Student's t-test). D Summery of tumor volume of mice which were measured every week (***P<0.001, Student's t-

test). E The expression of P27/P21 was also measured using IHC in xenograft (**P<0.01, Student's t-test, Magnification,×40). F and G The verification of miR-222-3p and miR-146a-5p in 4 pairs of xenograft tumors transfected with circFAM114A2 or vector detected by qRT-PCR (*P<0.05, **P<0.01, Student's t-test). H. The level of P27/P21 expression in 4 pairs of xenograft tumors transfected with circFAM114A2 or vector was detected by western blot.

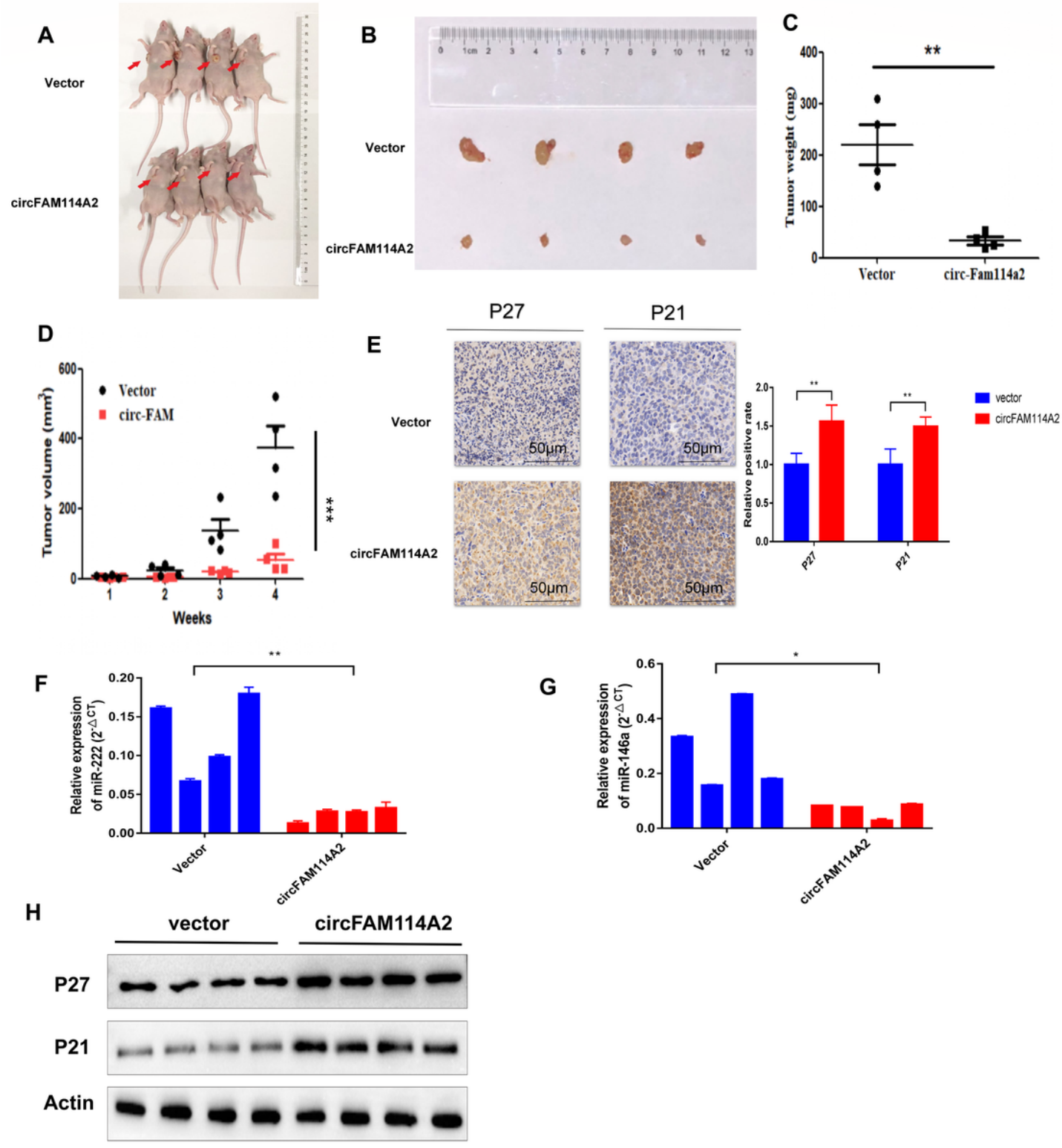

Figure 7

CircFAM114A2 suppressed tumor formation of xenograft in nude mice. A Representative image of the nude mice injected with circFAM114A2 or vector transfection T24 cells (n=4). B Representation picture of tumor formation of xenograft in nude mice injected with circFAM114A2 or vector transfection T24 cells (n=4). C Weights of tumors in two groups were measured using electronic scales (**P<0.01, Student's t-test). D Summery of tumor volume of mice which were measured every week (***P<0.001, Student's t-test). E The expression of P27/P21 was also measured using IHC in xenograft (**P<0.01, Student's t-test, Magnification,×40). F and G The verification of miR-222-3p and miR-146a-5p in 4 pairs of xenograft tumors transfected with circFAM114A2 or vector detected by qRT-PCR (*P<0.05, **P<0.01, Student's t-test). H. The level of P27/P21 expression in 4 pairs of xenograft tumors transfected with circFAM114A2 or vector was detected by western blot.

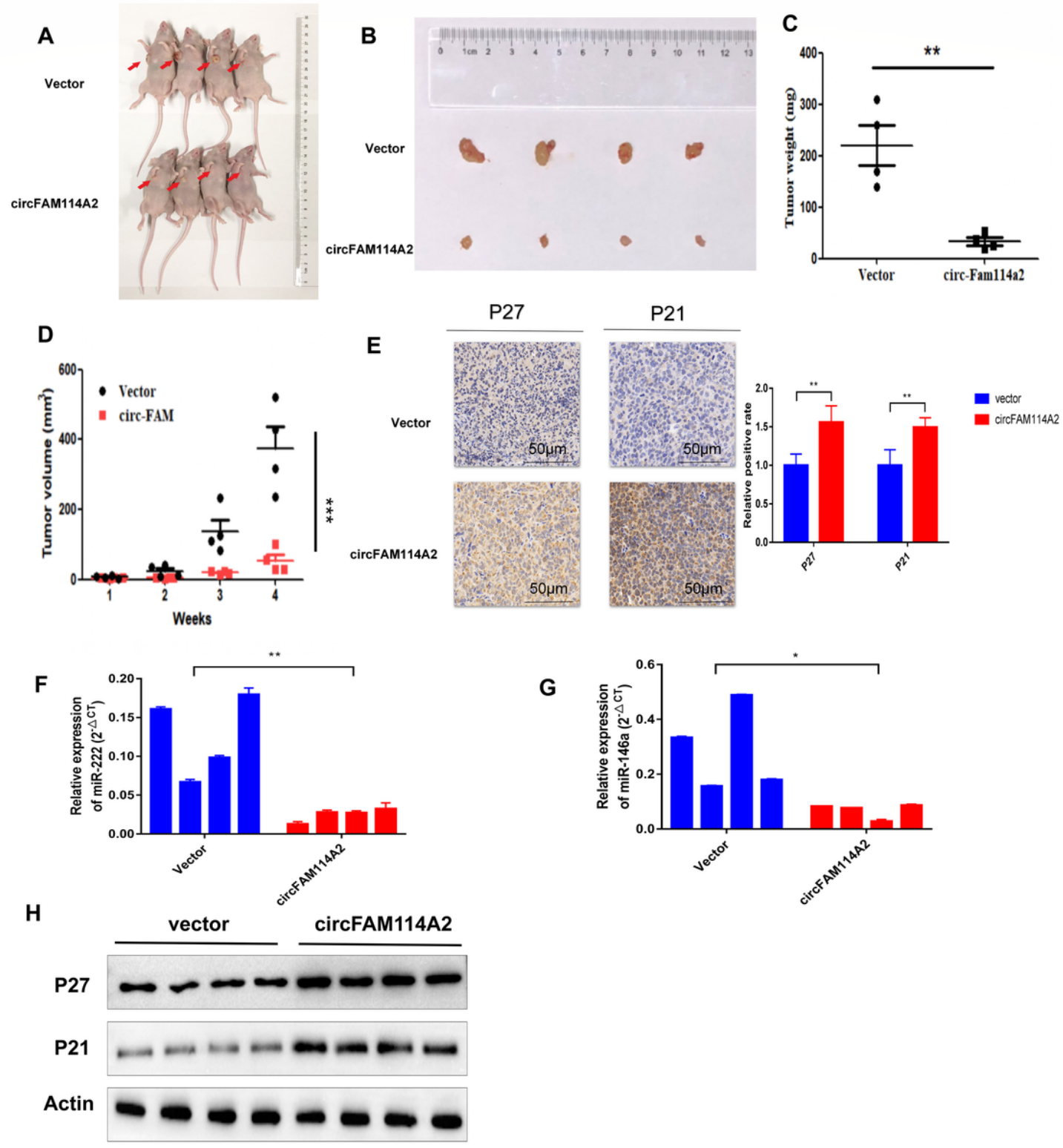

Figure 7

CircFAM114A2 suppressed tumor formation of xenograft in nude mice. A Representative image of the nude mice injected with circFAM114A2 or vector transfection T24 cells (n=4). B Representation picture of tumor formation of xenograft in nude mice injected with circFAM114A2 or vector transfection T24 cells (n=4). C Weights of tumors in two groups were measured using electronic scales (**P<0.01, Student's t-test). D Summery of tumor volume of mice which were measured every week (***P<0.001, Student's t-

test). E The expression of P27/P21 was also measured using IHC in xenograft (**P<0.01, Student's t-test, Magnification,×40). F and G The verification of miR-222-3p and miR-146a-5p in 4 pairs of xenograft tumors transfected with circFAM114A2 or vector detected by qRT-PCR (*P<0.05, **P<0.01, Student's t-test). H. The level of P27/P21 expression in 4 pairs of xenograft tumors transfected with circFAM114A2 or vector was detected by western blot.

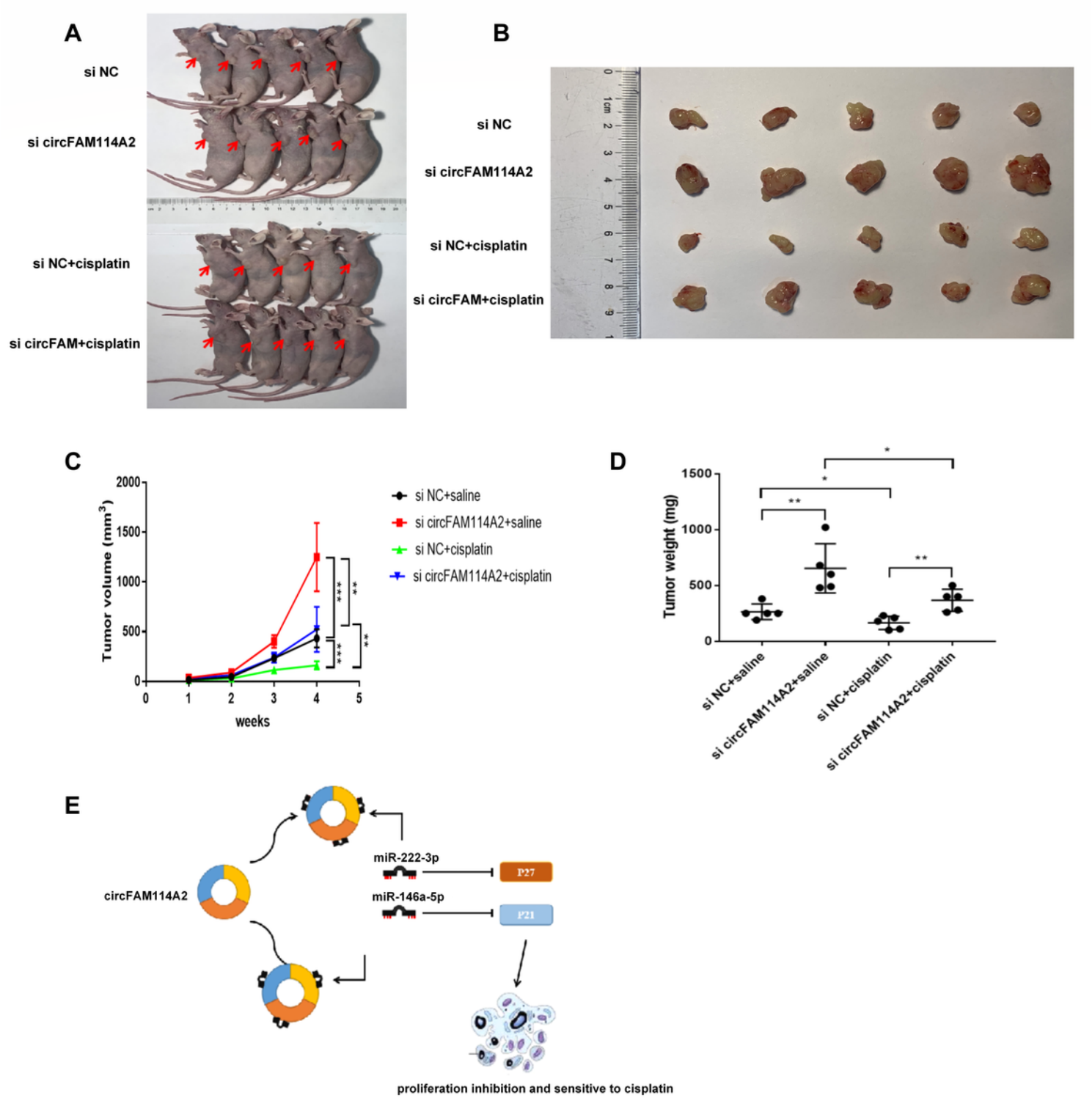

Figure 8

CircFAM114A2 promoted cisplatin sensitivity in nude mice. A Representative image of the nude mice injected with si circFAM114A2 or si NC transfection T24 cells, which treated with cisplatin or saline (n=5). B Representation picture of tumor formation of xenograft in nude mice injected with si circFAM114A2 or si NC transfection T24 cells, which treated with cisplatin or saline (n=5). C Summery of tumor volume of four group of nude mice which were measured every week (**P<0.01, ***P<0.001, Student's t-test). D Weights of tumors in four groups were measured using electronic scales (*P<0.05, **P<0.01, Student's t-test). E Mode pattern of the circFAM114A2-miR-222-3p/miR-146a-5p-P27/P21 regulatory network. Data are mean±SD, n=3

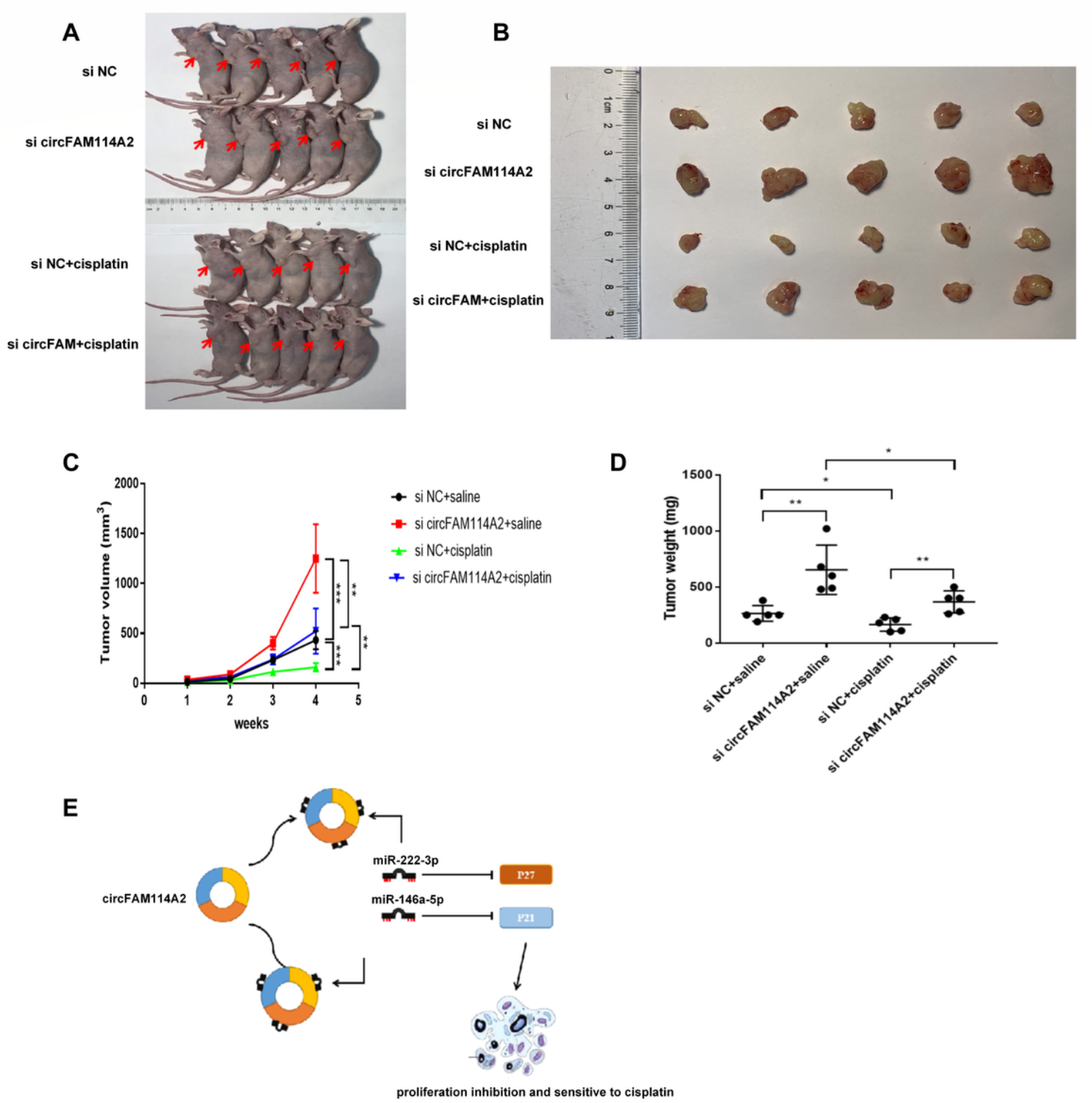

Figure 8

CircFAM114A2 promoted cisplatin sensitivity in nude mice. A Representative image of the nude mice injected with si circFAM114A2 or si NC transfection T24 cells, which treated with cisplatin or saline (n=5). B Representation picture of tumor formation of xenograft in nude mice injected with si circFAM114A2 or si NC transfection T24 cells, which treated with cisplatin or saline (n=5). C Summery of tumor volume of four group of nude mice which were measured every week (**P<0.01, ***P<0.001, Student's t-test). D Weights of tumors in four groups were measured using electronic scales (*P<0.05, **P<0.01, Student's t-test). E Mode pattern of the circFAM114A2-miR-222-3p/miR-146a-5p-P27/P21 regulatory network. Data are mean±SD, n=3

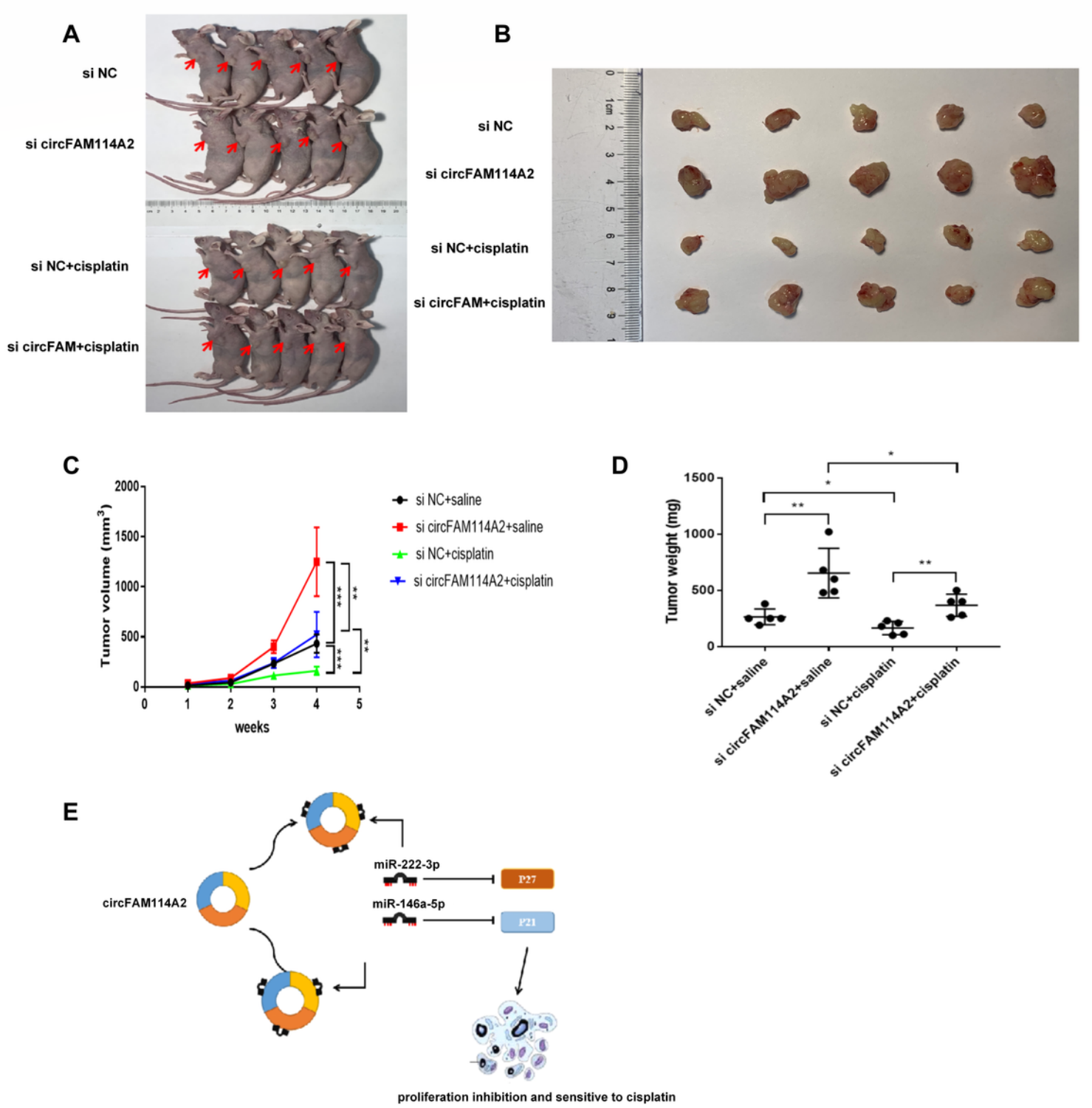

Figure 8

CircFAM114A2 promoted cisplatin sensitivity in nude mice. A Representative image of the nude mice injected with si circFAM114A2 or si NC transfection T24 cells, which treated with cisplatin or saline (n=5). B Representation picture of tumor formation of xenograft in nude mice injected with si circFAM114A2 or si NC transfection T24 cells, which treated with cisplatin or saline (n=5). C Summery of tumor volume of four group of nude mice which were measured every week (**P<0.01, ***P<0.001, Student's t-test). D

Weights of tumors in four groups were measured using electronic scales (*P<0.05, **P<0.01, Student's t-test). E Mode pattern of the circFAM114A2-miR-222-3p/miR-146a-5p-P27/P21 regulatory network. Data are mean±SD, n=3

Supplementary Files

This is a list of supplementary files associated with this preprint. Click to download.

- Additionaltable1.docx
- Additionaltable1.docx
- Additionaltable1.docx
- Additionaltable2.docx
- Additionaltable2.docx
- Additionaltable2.docx
- Additionalfigure1.tif
- Additionalfigure1.tif
- Additionalfigure1.tif
- Additionalfigure2.tif
- Additionalfigure2.tif
- Additionalfigure2.tif
- Additionalfigure3.tif
- Additionalfigure3.tif
- Additionalfigure3.tif
- Additionalfigure4.tif
- Additionalfigure4.tif
- Additionalfigure4.tif
- Additionalfigure5.tif
- Additionalfigure5.tif
- Additionalfigure5.tif
- Additionalfigure6.tif
- Additionalfigure6.tif
- Additionalfigure6.tif